

Alma Mater Studiorum Università di Bologna
Archivio istituzionale della ricerca

Protective effects of chrysin against the neurotoxicity induced by aluminium: In vitro and in vivo studies

This is the final peer-reviewed author's accepted manuscript (postprint) of the following publication:

Published Version:

Campos H.M., da Costa M., da Silva Moreira L.K., da Silva Neri H.F., Branco da Silva C.R., Pruccoli L., et al. (2022). Protective effects of chrysin against the neurotoxicity induced by aluminium: In vitro and in vivo studies. TOXICOLOGY, 465, 1-13 [10.1016/j.tox.2021.153033].

Availability:

This version is available at: <https://hdl.handle.net/11585/843655> since: 2024-09-04

Published:

DOI: <http://doi.org/10.1016/j.tox.2021.153033>

Terms of use:

Some rights reserved. The terms and conditions for the reuse of this version of the manuscript are specified in the publishing policy. For all terms of use and more information see the publisher's website.

This item was downloaded from IRIS Università di Bologna (<https://cris.unibo.it/>).
When citing, please refer to the published version.

(Article begins on next page)

This is the final peer-reviewed accepted manuscript of:

Campos, H.M., da Costa, M., da Silva Moreira, L.K., da Silva Neri, H.F., Branco da Silva, C.R., Pruccoli, L., dos Santos, F.C.A., Costa, E.A., Tarozzi, A., Ghedini, P.C., 2022. Protective effects of chrysin against the neurotoxicity induced by aluminium: In vitro and in vivo studies. *Toxicology* 465, 153033.

<https://doi.org/10.1016/j.tox.2021.153033>

The final published version is available online at:

<https://doi.org/10.1016/j.tox.2021.153033>

Terms of use:

Some rights reserved. The terms and conditions for the reuse of this version of the manuscript are specified in the publishing policy. For all terms of use and more information see the publisher's website.

This item was downloaded from IRIS Università di Bologna (<https://cris.unibo.it/>)

When citing, please refer to the published version.

**Protective Effects of Chrysin against the Neurotoxicity Induced by Aluminium: In Vitro
and In Vivo Studies**

Hericles Mesquita Campos ^a, Michael da Costa ^a, Lorrane Kelle da Silva Moreira ^a, Hiasmin
Franciely da Silva Neri ^a, Cinthia Rio Branco da Silva ^b, Letizia Pruccoli ^c, Fernanda Cristina
Alcantara dos Santos ^b, Elson Alves Costa ^a, Andrea Tarozzi ^c, Paulo César Ghedini ^{a, *}

^a Department of Pharmacology, Institute of Biological Sciences, Federal University of Goiás,
Goiania, GO, Brazil.

^b Department of Histology, Embryology and Cell Biology, Institute of Biological Sciences,
Federal University of Goiás, Goiania, GO, Brazil.

^c Department for Life Quality Studies, University of Bologna, Rimini, Italy.

* Corresponding author: Biochemical and Molecular Pharmacology Laboratory, Institute of
Biological Sciences, Federal University of Goiás, Cep 74690-900, Goiania, GO, Brazil.

E-mail: pcghedini@gmail.com; phone +55 62 3521-1725

Abstract

Chronic exposure to aluminium (Al) can contribute to the progression of several neurological and neurodegenerative diseases. Al is a metal that promotes oxidative damage leading to neuronal death in different brain regions with behavior, cognition, and memory deficits. Chrysin is a flavonoid found mainly in honey, passion fruit, and propolis with antioxidant, anti-inflammatory, and cytoprotective properties. In this study, we used an integrated approach of *in vitro* and *in vivo* studies to evaluate the antioxidant and neuroprotective effects of chrysin against the neurotoxicity elicited by aluminium chloride (AlCl₃). In *in vitro* studies, chrysin (5 µM) showed the ability to counteract the early oxidative stress elicited by tert-butyl hydroperoxide, an oxidant that mimics the lipid peroxidation and Fenton reaction in presence of AlCl₃ as well as the late necrotic death triggered by AlCl₃ in neuronal SH-SY5Y cells. *In vivo* studies in a mouse model of neurotoxicity induced by chronic exposure to AlCl₃ (100 mg/kg/day) for ninety days then corroborated the antioxidant and neuroprotective effect of chrysin (10, 30, and 100 mg/kg/day) using the oral route. In particular, chrysin reduced the cognitive impairment induced by AlCl₃ as well as normalized the acetylcholinesterase and butyrylcholinesterase activities in the hippocampus. In parallel, chrysin counteracted the oxidative damage, in terms of lipid peroxidation, protein carbonylation, catalase, and superoxide dismutase impairment, in the brain cortex and hippocampus. Lastly, necrotic cells frequency in the same brain regions was also decreased by chrysin. These results highlight the ability of chrysin to prevent the neurotoxic effects associated with chronic exposure to Al and suggest its potential use as a food supplement for brain health.

Keywords: Aluminium; neurotoxicity, oxidative stress; antioxidant; chrysin.

1. Introduction

Aluminum (Al) is the third most abundant element in the earth's crust and occurs naturally in the environment, foodstuffs, and drinking water. According to the European Food Safety Authority (EFSA), the human tolerable weekly intake is 1 mg Al/kg body weight (BW) in a 60-kg adult. However, in some individuals this intake is exceeded as a result of estimated daily alimentary aluminum exposure of 1.6–13 mg (0.2–1.5 mg/kg BW/week) (Klotz et al., 2017).

The toxic effects of this metal occur through its accumulation over time and several sources contribute to Al exposure in humans, such as industrial areas (0.04 to 1.4 mg/m³/day), natural water (different cities around the world have reported concentrations as high as 0.4–2.7 mg/L), foods (3–11 mg/kg/day), drugs such as antacid (104–208 mg of Al per tablet) and aspirin (10 – 20 mg of Al per tablet), and cosmetics (10.98 – 694.5 mg/kg in lipsticks) (Krewski et al., 2007; Exley, 2013; Borowska & Brzóska, 2015).

Among the different forms of Al, the ionic form of Al³⁺ can exert various cytotoxic effects through its ability to induce the formation of reactive oxygen species, oxidative damage, and neuronal death (Willhite et al., 2014). Al³⁺ can also cross the blood-brain barrier and accumulate in various human brain regions, suggesting the contribution of Al to the progression of neurological and neurodegenerative diseases, including Alzheimer's disease (AD), dialysis dementia syndrome, autism spectrum disorder, multiple sclerosis, and epilepsy (Lukiw et al., 2018; Exley and Mold, 2019). In this regard, the chronic accumulation of Al in the brain induces deregulation of gene expression in neurons, gliosis, neuronal death, and functional decline resulting in deficits in cognition, memory, and behavior (Lukiw et al., 2018).

Although Al is a low redox metal, considerable evidence supports its pro-oxidant activity at the brain level (Maya et al., 2016; Garza-Lombó et al., 2018). Al can bind to brain phospholipids, which contain polyunsaturated fatty acids vulnerable to the oxidizing action of

1 reactive oxygen species (ROS), including hydrogen peroxide (H₂O₂), superoxide (O₂⁻), and
2 hydroxyl (OH[·]) radical (Yuan et al., 2012). In particular, Al can strengthen the iron (Fe²⁺)-
3 initiated lipid peroxidation in the Fenton reaction, which causes Fe³⁺ formation and ROS
4 production. Further, O₂⁻ is neutralized by Al³⁺ to form an Al-O₂⁻ complex, which increases
5 the oxidative capacity of O₂⁻ (Ruipérez et al., 2012). In this context, the neurobehavioral
6 deficits, such as defects in memory and motor functions, elicited by chronic exposure to Al
7 also reflect the ability of this metal to promote oxidative stress and neurodegeneration in brain
8 regions rich in polyunsaturated fatty acids, including the cortex and hippocampus (Drobyshev
9 et al., 2018; Farhat et al., 2019). Recent studies also show a cross talk between oxidative stress
10 and neuroinflammation in neurodegeneration elicited by Al chronic exposure (Maya et al.,
11 2016). The neuroinflammatory response triggered by oxidative stress can contribute to
12 cognitive impairments through neuropathological and neurochemical changes in the cortex and
13 hippocampus (Fernandes et al., 2020).

14 The use of natural antioxidants as potential therapeutics is a challenging area of
15 neuroscience research (Tal et al., 2016). Among natural antioxidants, the chrysin is a flavonoid
16 (5,7-dihydroxyflavone) found mainly in mushrooms (*Lactarius deliciosus* - 0.17 mg/kg, *Suillus*
17 *bellinii* - 0.34 mg/kg), passion fruit (*Passiflora ocreata* - 40 mg/mL, *Passiflora edulis*, and
18 *Passiflora caerulea* L. - 0.012 - 0.25 mg/mL), propolis (28 mg/mL), and in honey (e.g. honey
19 of honeydew - 0.10 mg/kg, and forest honeys- 5.3 mg/kg) (Hadjmohammadi et al., 2010;
20 Kalogeropoulos et al., 2013; Nabavi et al., 2015; El-Askary et al., 2017; Mani and Natesan,
21 2018). In addition, marketed tablets/capsules may include 300-800 mg of chrysin (Nabavi et
22 al., 2015; Manzolli et al., 2015; Mohos et al., 2018; Mohos et al., 2020).

23 Food supplementation with honey showed the ability to decrease both the brain lipid
24 peroxidation and neuronal death in the hippocampus CA1 in rats, while propolis oil improved
25 the behavior impairment of anxiety and depression in a similar rodent model (Reis et al., 2014;

Sairazi et al., 2017). These evidences suggest the ability of natural antioxidants present in honey and propolis, such as chrysin, to cross the blood-brain barrier (BBB) and affect the oxidative stress on the central nervous system (CNS) level. In this regard, an *in silico* approach to predict the pharmacokinetics of chrysin by the SwissADME web tool reveal its good overall drug-likeness profile including high gastrointestinal absorption and BBB permeant (Daiana and Zoete, 2016; Daiana et al., 2016).

Chrysin showed antioxidant and neuroprotective effects against cognitive decline in a rat model of diabetes and neurodegeneration induced by 6-hydroxydopamine in a mouse model of Parkinson's disease (Li et al., 2014; Manzolli et al., 2015; Nabavi et al., 2015). However, the neuroprotective effects of chrysin against the neurotoxicity evoked by Al remain unknown.

In this study, we used an *in vitro* experimental approach to evaluate: 1) the antioxidant effects of chrysin against the oxidative stress induced by various oxidants and Fenton reaction promoted by aluminium chloride (AlCl_3) in neuronal SH-SY5Y cells, as well as the ability of chrysin to counteract both the oxidative stress and inflammation evoked by lipopolysaccharides (LPS) in microglial THP-1 cells; 2) the neuroprotective effects of chrysin against the neurotoxicity in terms of cytostatic effects and necrosis elicited by AlCl_3 in neuronal SH-SY5Y cells; 3) we, then, assessed the antioxidant and neuroprotective activity of chrysin in a mouse model of neurotoxicity induced by chronic exposure to AlCl_3 . Chrysin was administered to mice using the oral route to explore its potential use as a food supplement for brain health.

2. Materials and Methods

2.1 Chemicals

AlCl_3 , iron sulfate (FeSO_4), chrysin (97% purity - Fig. 1), hydrogen peroxide (H_2O_2), tert-butyl hydroperoxide (t-BuOOH), acetylthiocholine (ATCh), 2,2'-azinobis-(3-ethylbenzothiazoline-6-sulfonic acid) ($\text{ABTS}^{\bullet+}$), butyrylthiocholine (BTCh), 2-7-

dichlorodihydrofluorescein diacetate (H2DCF-DA), 5,5'-dithiobis-(2-nitrobenzoic acid) (DTNB), malondialdehyde (MDA), epinephrine bitartrate, 2,4-dinitrophenylhydrazine (DNPH), sodium dodecyl sulfate (SDS), eosin, hematoxylin, and serum albumin (BSA) were obtained from Sigma Chemical (St. Louis, MO, USA). All other chemicals were obtained in an analytical grade or from standard commercial suppliers.

2.2 In vitro tests

2.2.1 Cell culture

Human neuronal SH-SY5Y cells were purchased from Lombardy and Emilia Romagna Experimental Zootechnic Institute (Italy). SH-SY5Y cells were routinely grown in Dulbecco's Modified Eagle Medium with phenol red supplemented with 10% fetal bovine serum, 2 mM L-glutamine, 50 U/mL penicillin, and 50 µg/mL streptomycin at 37 °C in a humidified incubator with 5% CO₂. For all experiments the SH-SY5Y cells were used below passage 12 to avoid phenotype changes and cellular senescence.

Human monocyte THP-1 cells were purchased from Cell bank Interlab Cell Line Collection (Italy). THP-1 cells were routinely grown in Roswell Park Memorial Institute (RPMI) 1640 Medium with phenol red supplemented with 10% fetal bovine serum, 2 mM L-glutamine, 50 U/mL penicillin, and 50 µg/mL streptomycin at 37 °C in a humidified incubator with 5% CO₂. THP-1 cells were differentiated into microglia-like cells with phorbol 12-myristate 13-acetate (PMA, 10 µg/ml) for 24 h at 37°C in 5% CO₂.

2.2.2 Neuronal viability

The neuronal viability was assessed using the tetrazolium salt colorimetric assay as previously described by Ortiz et al., 2020. Briefly, SH-SY5Y cells were seeded in a 96 well plate at 2×10^4 cells/well, incubated for 24 h, and subsequently treated with various

1 concentrations of chrysin (1.25 – 40 μ M) for 24 h at 37°C in 5% CO₂. The cell viability, in
2 terms of mitochondrial metabolic function, was evaluated by the reduction of 3-(4,5-dimethyl-
3 2-thiazolyl)-2,5-diphenyl2H-tetrazolium bromide (MTT) to its insoluble formazan. The
4 treatment was replaced with MTT in HBSS [0.5 mg/mL] for 1 h at 37°C in 5% CO₂. After
5 washing with HBSS, formazan crystals were dissolved in isopropanol. The amount of formazan
6 was measured (570 nm, reference filter 690 nm) using a multilabel plate reader (VICTOR™
7 X3, PerkinElmer, Waltham, MA, USA). The quantity of formazan was directly proportional to
8 the number of living cells. Data are expressed as percentages of neuronal viability with control
9 taken as 100% viability.
10
11
12
13
14
15
16
17
18
19
20
21
22
23

24 **2.2.3 Antioxidant activity in neuronal SH-SY5Y cells**

25 The antioxidant activity of chrysin was evaluated in neuronal SH-SY5Y cells as
26 previously described by Tarozi et al., 2012. Briefly, cells were seeded in a 96 well plate at 3
27 $\times 10^4$ cells/well, incubated for 24 h, and subsequently loaded with the fluorescent probe
28 H₂DCF-DA (10 μ g/mL) for 30 min at room temperature. At the end of incubation, cells were
29 treated with various concentrations of chrysin (1.25 – 5 μ M) and H₂O₂ or *t*-BuOOH (100 μ M)
30 for 30 min. The intracellular ROS formation was measured (excitation at 485 nm and emission
31 at 535 nm) using a VICTOR™ X3 multilabel plate reader. Data are expressed as Arbitrary Unit
32 of Fluorescence (AUF).
33
34
35
36
37
38
39
40
41
42
43
44
45

46 The total antioxidant activity (TAA) was measured on both the cytosolic and membrane
47 enriched fractions as previously reported by Tarozi et al., 2014. Briefly, SH-SY5Y cells were
48 seeded in cultures dishes at 4×10^6 cells/dish for 24 h at 37°C in 5% CO₂. At the end of
49 incubation, cells were treated for 2 h with chrysin (5 μ M). After washing with cold phosphate
50 buffer saline (PBS), cells were collected in 1 ml of PBS and centrifuged for 10 min at 10,000
51 g at 4 °C. The supernatant was removed and after washing with PBS, the pellet was finally
52
53
54
55
56
57
58
59
60
61
62
63
64
65

1 reconstituted in 600 μ l of 0.05 % Triton X-100. Cells were then homogenized and allowed to
2 stand at 4 °C for 30 min. Cytosolic and membrane enriched fractions were subsequently
3
4 separated by centrifugation at 15,000 g for 15 min at 4 °C. TAA in cell fractions was
5
6 determined by the decoloration of the radical cation of ABTS^{•+}, in terms of quenching of
7
8 absorbance at 740 nm. Data for each sample were compared with the concentration-response
9
10 curve of a standard antioxidant, such as Trolox (a water-soluble vitamin E analog) and
11
12 expressed as μ mol of Trolox Equivalent Antioxidant Activity per mg of protein (μ molTE/mg
13
14 protein).
15
16
17
18

19 The antioxidant activity of chrysin against the oxidative stress induced by the synergic
20
21 effect of Fenton reaction and AlCl₃ was evaluated in neuronal SH-SY5Y cells. Briefly, cells
22
23 were seeded in a 96 well plate at 3×10^4 cells/well, incubated for 24 h, and subsequently loaded
24
25 with the fluorescent probe H₂DCF-DA (10 μ g/mL) for 30 min at room temperature. At the end
26
27 of incubation, cells were first treated for 15 min with FeSO₄/H₂O₂/AlCl₃ (50 μ M/200 μ M/50
28
29 μ M) and then treated for 15 min with chrysin (5 μ M). The ROS formation was measured
30
31 (excitation at 485 nm and emission at 535 nm) using a VICTOR™ X3 multilabel plate reader.
32
33 Data are expressed as AUF.
34
35
36
37
38
39
40

41 **2.2.4 Antioxidant activity in microglial THP-1 cells**

42

43 The antioxidant activity of chrysin against the oxidative stress induced by *t*-BuOOH
44
45 was evaluated in microglial THP-1 cells. Briefly, THP-1 cells were seeded in cultures dishes
46
47 at 2.5×10^6 cells/dish and incubated for 24 h with PMA (10 μ g/ml) for differentiation to
48
49 microglial-like cells. After the differentiation, cells were incubated with the fluorescent probe
50
51 H₂DCF-DA (10 μ g/mL) for 30 min at room temperature. At the end of incubation, cells were
52
53 treated with various concentrations of chrysin (1.25 – 5 μ M) and *t*-BuOOH (100 μ M) for 30
54
55
56
57
58
59
60
61
62
63
64
65

min. The ROS formation was measured (excitation at 485 nm and emission at 535 nm) using a VICTOR™ X3 multilabel plate reader. Data are expressed as AUF.

The antioxidant activity of chrysin against the oxidative stress induced by lipopolysaccharides (LPS) was evaluated in microglial THP-1 cells. Briefly, cells were seeded in cultures dishes at 2.5×10^6 cells/dish, incubated for 24 h with PMA (10 µg/mL) and subsequently, treated for 24 h with chrysin (5 µM) and LPS (1µg/mL). At the end of incubation, cells were loaded with the fluorescent probe H₂DCF-DA (10 µg/mL) for 30 min at room temperature. The ROS formation was measured (excitation at 485 nm and emission at 535 nm) using a VICTOR™ X3 multilabel plate reader. Data are expressed as AUF.

2.2.5 Anti-inflammatory activity in microglial THP-1 cells

The anti-inflammatory activity of chrysin in microglial THP-1 activated by LPS was performed as previously described by Di Martino et al., 2020. Briefly, THP-1 cells were seeded in 60 mm dishes at 2.5×10^6 cells/dish, incubated for 24 h with PMA (10 µg/mL) and subsequently, treated for 24 h with chrysin (5 µM) and LPS (1µg/mL). Afterward, the cell suspension was pelleted, and RNA was extracted by the PureLink RNA Mini Kit (Life Technologies, Carlsbad, CA, USA) according to the manufacturer's guidelines. A total of 1 µg of RNA were used to synthesize cDNA using the SuperScript VILO MasterMix (Invitrogen, Carlsbad, CA, USA). Quantitative RT-PCR was carried out using SYBR Select Master Mix (Invitrogen), and relative normalized expression was calculated by comparing the cycle threshold (Ct) of the target gene (Inducible nitric oxide synthase, iNOS; Interleukin 1 beta; IL-1β; Tumour Necrosis Factor-alpha; TNF-α) to that of the reference genes β-Actin and glyceraldehyde-3-phosphate dehydrogenase protein (GAPDH, Life Technologies). All reactions had three technical replicates, and each condition had three biological replicates.

Relative quantification was calculated according to the $\Delta\Delta C_t$ method ($2^{-\Delta\Delta C_t}$) with untreated cells as control. Primer sequences used in this study are listed in Table 1.

2.2.6 Neuroprotective activity in neuronal SH-SY5Y cells

The neuroprotective activity of chrysin was evaluated in neuronal SH-SY5Y cells in terms of cytostatic effect and necrosis using trypan blue and propidium iodide (PI), respectively, as previously described by Pruccoli et al., 2020. Cells were seeded in 60 mm dishes at 1×10^6 cells/dish, incubated for 24 h, and subsequently treated for 24 h with chrysin (5 μ M) and $AlCl_3$ (50 μ M). At the end of incubation, cells were collected and the cytostatic effect, in terms of the number of total cells, was detected by using trypan blue (1:10). In parallel, cells were loaded with PI (25 μ g/mL) for 5 min at room temperature. The necrosis was detected by using an inverted fluorescence microscope (Eclipse Ti-E, Nikon Instruments Spa, Florence, Italy). The total cells were counted in a bright field, then only the red necrotic cells were counted using TRITC filters (EX 535/50, BS 575, EM 590LP). Data are expressed as a percentage of necrotic cells versus total cells.

2.3 In vivo tests

2.3.1 Animals

Experiments were conducted using male Swiss mice (25 – 30 g) about two months old. Animals were maintained at a stable temperature of 22 ± 2 °C and a controlled 12 hours light/dark cycle, with free access to food and water. All manipulations were carried out between 08:00 and 16:00. All the protocols and experimentations were approved by the Brazilian College of Animal Experimentation (COBEA) and were approved by the local Ethics in Research Committee (protocol number: 056/2016) of the Federal University of Goiás (UFG).

2.3.2 Experimental design

The animals were randomized into five groups (n = 14 – 16): control; aluminum chloride 100 mg/kg (AlCl₃) dissolved in water; chrysin 10 mg/kg (Chrysin 10); chrysin 30 mg/kg (Chrysin 30) and chrysin 100 mg/kg (Chrysin 100). The control group received water, while all other groups received AlCl₃ 100 mg/kg/day for 90 days (Treatment 1). On the 46th day, the control and AlCl₃ groups received normal saline (adjusted pH 7.4) while all the other groups received chrysin until the 90th day (Treatment 2). All treatments were administered daily by gavage at a volume of 10 µL/1 g.

The chrysin doses were chosen based on a previous work of He et al., 2012 and Sarkaki et al., 2019. The Al dose and treatment periods were chosen based on previous work of our group (Oliveira et al., 2018; Thomaz et al., 2018).

At the end of the behavioral tests, the number of animals per group was subdivided for the biochemical assays (n = 8) and the histopathological and morphometric analysis (n = 5).

2.4 Behavioral tests

2.4.1 Open field test (OFT)

Exploratory activity was measured in the OFT (Montgomery, 1956) at protocol day 90, previously to the memory task. The floor of the open field was divided into nine squares. Each animal was placed individually in the center of the arena, and the number of segments crossed (four-paw criterion) was recorded in a 5 min session.

2.4.2 Chimney test (CT)

Locomotor activity was measured in the CT (Boissier, 1960) also at protocol day 90. This test consisted of evaluating the ability of animals to climb back up through an acrylic tube. The animals were introduced in the tube horizontally, and when they reach the opposite

extremity, the tube was put in the vertical position, and the activity of the animals to climb for 30 sec was observed.

2.4.3 Step-down avoidance test (SDPAT)

The SDPAT has been used to study nonspatial long-term memory (Kameyama et al., 1986). The apparatus consisted of a single box where the floor was made of a metal grid connected to a shock scrambler. A safe platform was also placed in the box. The training session (acquisition) day 91, consisted in putting the mice gently on the platform and upon stepping with four paws onto the grid floor, an electric shock of 0.5 mA/s was delivered. The latency of the step-down motion into the grid was recorded in the training session. Some seconds later (~5), the mouse was removed from the SDPAT apparatus and returned to its home cage. The retention trial was performed 24 h after training on day 92. For this, mice were placed on the platform, but no shock was given when they went down. The criterion for learning was taken as an increase in the transfer latency time on the retention trial as compared to the acquisition trial. Therefore, short transfer latencies indicate poor retention. The box was illuminated throughout the experimental period.

2.5 Ex vivo tests

2.5.1 Tissue collection and preparation

Twenty-four hours after the last behavioral test, the animals were anesthetized intraperitoneally with ketamine and xylazine hydrochloride. They were subsequently sacrificed by decapitation and the brain cortex and hippocampus were removed and dissected. Cerebral tissue samples were homogenized in 0.1 mol/L potassium phosphate buffer (KPB), pH = 7.4 in a 1:10 (w/v) ratio. The homogenate was then centrifuged at 8000 x g for 10 min to yield the low-speed supernatant (S1) fractions that were used in the assays.

2.6 Biochemical assays

2.6.1 Cholinesterase (ChEs) activity

Enzyme activities were carried out according to the method of Ellman et al., 1961. The S1 fractions were incubated with 0.3 mmol/L DTNB, and the enzymatic reaction was initiated by the addition of 0.45 mmol/L of ATCh and BTCh as the substrate for AChE and BChE, respectively. Enzyme activities were spectrophotometrically measured at 412 nm for 3 min. Results are expressed in $\mu\text{mol ACTh/min/mg protein}$ and $\mu\text{mol BCTh/min/mg protein}$ for AChE and BChE, respectively.

2.6.2 Lipid peroxidation (LPO) levels

For LPO measurement the method of thiobarbituric acid reactive substances (TBARS) was used. The TBARS estimation was spectrophotometrically performed following the method described by Ohkawa et al., 1979, with some modifications. The S1 fractions were incubated with thiobarbituric acid, acetic acid (pH 3.4), and SDS at 95 °C for 60 min. The reaction product was determined at 532 nm. For the interpretation of the results, a MDA curve was performed and the data are expressed as equivalents of MDA in nmol/mg protein.

2.6.3 Carbonylated protein (CP) levels

Protein carbonyl derivatives were measured following the method described by Levine et al., 1990, with some modifications. The S1 fractions were incubated with DNPH prepared in 2 mol/L HCl. The mixture was kept in the dark for 1 h and vortexed each 15 min. Denaturation buffer, ethanol, and hexane were then added to each tube and the final mixture was vortexed for 40 sec and centrifuged at 3000 x g for 10 min. The supernatant obtained was discarded. The pellet was washed with ethanol-ethyl acetate (1:1 v/v) and re-suspended in a

denaturation buffer. The sample was vortexed for 5 min and was used to measure absorbance at 370 nm. Results are expressed as nmol of carbonyl content/mg protein.

2.6.4 Superoxide dismutase (SOD) activity

The brain cortex and hippocampus SOD activities were spectrophotometrically determined according to the method of Misra and Fridovich, 1972. The principle of this method is the ability of the superoxide dismutase enzyme to inhibit the autoxidation of epinephrine. The S1 fractions were incubated with 60 mmol/L of epinephrine bitartrate (pH 10) and the sample color intensity was measured at 480 nm. The enzymatic activity was expressed in units (U) of SOD/mg of protein.

2.6.5 Catalase (CAT) activity

The brain cortex and hippocampus CAT activities were spectrophotometrically determined by the H₂O₂ decomposition at 240 nm according to the method described by Aebi, 1984, with some modifications. The S1 fractions were incubated with 86 mmol/L H₂O₂ and sodium phosphate buffer (pH 7.0). The enzymatic activity was expressed in U of CAT/mg of protein. One U of enzyme thus decomposed one μ mol of H₂O₂/min at pH 7.0 at 25 °C.

2.6.6 Protein content determination

Total protein concentration was measured by the method described by Bradford, 1976 using bovine albumin serum as the standard.

2.7 Histopathological and morphometric analysis

The brain cortex and hippocampus were fixed by immersion in 4 % paraformaldehyde (buffered in 0.1 M phosphate, pH 7.2) for 24 h. The tissues were then dehydrated through a

crescent ethanol series, clarified in xylol, embedded in paraplast (Histosec, Merck, Darmstadt, Germany), and sectioned at 5 μ m on a Leica microtome (Leica RM2155, Nussloch, Germany). Sections were stained by thionine acetate and analyzed in a Zeiss Axioscope A1 light microscope (Zeiss, Germany). Morphometric analysis was performed to quantify the neurodegeneration in terms of the percentage (%) of eosinophilic neurons (necrosis-like cells) in the brain cortex and hippocampus (CA1 area). For this, 30 photomicrographic fields were obtained (6 fields/animal, n = 5 animals/group). The percentage (%) of necrotic neurons was obtained to the total number of neurons per photomicrographic field. All analyses were conducted using Image Pro-Plus program version 6.1 (Media Cybernetics Inc., Silver Spring, MD, USA).

2.8 Data presentation and statistical analysis

All experiments results are given as the mean (s) \pm standard error mean (SEM). Statistical analyses were performed using Student t-test or one-way ANOVA followed by Tukey's multiple comparisons test, Dunnett's test, Bonferroni's test, or Student's t-test as appropriate. Values of $p < 0.05$ were considered statistically significant. Calculations were performed using the software GraphPad Prism 8.0. San Diego, CA USA. (<https://www.graphpad.com>).

3. Results

3.1 In vitro studies

3.1.1 Neurotoxicity

The cytotoxicity of chrysin was evaluated in neuronal SH-SY5Y cells to define the range of concentrations not associated with toxicity. After 24 h of treatment with various concentrations of chrysin (1.25 – 40 μ M), the neuronal viability was measured using MTT

assay. As reported in Fig. 2A, the treatment with concentrations up to 5 μ M did not affect neuronal viability. Therefore, we selected the range of 1.25 – 5 μ M for the following experiments.

3.1.2 Antioxidant activity in neuronal SH-SY5Y and microglial THP-1 cells

The antioxidant activity of chrysin was first evaluated in neuronal SH-SY5Y cells against the ROS formation induced by H_2O_2 . After 30 min of treatment with chrysin (1.25 – 5 μ M) and H_2O_2 (100 μ M), the ROS formation was detected using the fluorescent probe H_2DCF -DA. As reported in Fig. 2B, chrysin significantly reduced the ROS formation in neuronal SH-SY5Y cells with all the concentrations used ($p = 0.0001$). The antioxidant activity was dose-correlated with EC_{50} (concentration in which the 50% of ROS formation is reduced) 4 μ M and maximum activity at 5 μ M (51% of ROS formation inhibition). The antioxidant activity of chrysin was then evaluated in both neuronal SH-SY5Y and microglial THP-1 cells against the ROS formation induced by t -BuOOH, which is known to generate ROS from lipid peroxidation (Christine et al., 2018). After 30 min of treatment with chrysin (1.25 – 5 μ M) and t -BuOOH (100 μ M), the ROS formation was detected using the fluorescent probe H_2DCF -DA. As reported in Fig. 3A, chrysin significantly decreased the ROS formation in neuronal SH-SY5Y cells with all the concentrations used ($p = 0.0011$). The antioxidant activity was dose-correlated with EC_{50} 2 μ M and maximum activity at 5 μ M (73% of ROS formation inhibition). To better evaluate the ability of chrysin to exert its antioxidant activity at the neuronal membrane level, we measured the TAA of cytosolic and membrane-enriched fractions of neuronal SH-SY5Y cells treated with 5 μ M of chrysin for 2 h. The membrane fractions, but not the cytosolic fractions, obtained from SH-SY5Y cells treated with chrysin showed a significant increase in TAA in comparison to untreated cells (untreated cells = 44.57 ± 0.3526 μ molTE/mg prot vs cells treated with chrysin = 68.90 ± 1.238 μ molTE/mg prot; $p = 0.0001$).

1 The antioxidant activity of chrysin was also evaluated in microglial THP-1 cells in the
2 same experimental conditions. As reported in Fig. 3B, Only the concentration of 5 μ M
3 significantly decreased the ROS formation induced by *t*-BuOOH in microglial THP-1 cells
4 (36% of ROS inhibition) ($p = 0.0011$). Driven by these results, the concentration of 5 μ M was
5 selected for the following experiments.
6
7
8
9
10

11 **3.1.3 Antioxidant and inflammatory activity in microglial THP-1 cells**

12
13
14
15
16 After 24 h of treatment with chrysin (5 μ M) and LPS (1 μ g/ml), the ROS formation was
17 detected using the fluorescent probe H₂DCF-DA. As reported in Fig. 4A, chrysin significantly
18 reduced the ROS formation evoked by 24 h of treatment with LPS ($p = 0.0020$). In parallel, the
19 expressions of pro-inflammatory cytokines iNOS, IL-1 β , and TNF α were evaluated in
20 microglial THP-1 cells after 24 h of treatment with chrysin and LPS by RT-PCR. As reported
21 in Fig. 4B-D, chrysin significantly decreased iNOS, IL-1 β , and TNF α expression at the
22 transcriptional level, suggesting its strong anti-inflammatory activity ($p = 0.0001$).
23
24
25
26
27
28
29
30
31
32

33 **3.1.4 Antioxidant activity against Fenton reaction/AlCl₃ in neuronal SH-SY5Y cells**

34
35
36 The antioxidant activity of chrysin was also evaluated against the pro-oxidant activity
37 of AlCl₃ on Fenton reaction in neuronal SH-SY5Y cells using the fluorescent probe H₂DCF-
38 DA. As shown in Fig. 5, the adding of AlCl₃ (50 μ M) to FeSO₄/H₂O₂ (50 μ M/200 μ M) reaction
39 for 15 min further increased the ROS formation in SH-SY5Y cells. In these experimental
40 conditions, chrysin (5 μ M) significantly abolished the pro-oxidant activity evoked by AlCl₃ (p
41 = 0.0001). In parallel, chrysin and AlCl₃ alone did not modify the basal level of ROS supporting
42 the ability of chrysin to counteract specific ROS generated by catalytic effects of AlCl₃ on
43 Fenton reaction.
44
45
46
47
48
49
50
51
52
53
54
55
56

57 **3.1.5 Neuroprotective activity in neuronal SH-SY5Y cells**

To determine the neuroprotective effects of chrysin in neuronal SH-SY5Y cells, the cytotoxicity induced by AlCl₃ in terms of cytostatic effect and necrosis was measured using trypan blue and PI, respectively. As reported in Fig. 6A, chrysin (5 μM) significantly counteracted the cytostatic effect induced by 24 h of treatment with AlCl₃ in terms of the number of total cells ($p = 0.0041$). In the same experimental conditions, chrysin significantly reduced the necrosis induced by AlCl₃ (Fig. 6B-C) ($p = 0.0007$).

3.2 *In vivo* studies

3.2.1 Behavioral test

3.2.1.1 OFT and CT

Mice performances in the OFT and CT are presented in Table 2. No effects on spontaneous locomotor ($p = 0.9662$) or exploratory ($p = 0.9518$) activities were observed due to any of the treatments.

3.2.1.2 SDPAT

Mice performance in the SDPAT is presented in Fig. 7. No difference among groups was observed in the transfer latency time in the acquisition phase. Statistical analysis yielded a significant difference among the groups ($p = 0.001$) in the retention phase. Post-hoc comparisons revealed that the AlCl₃ group presented a lower transfer latency time (~87%) than the control group. Chrysin treatment at all tested doses (10, 30 and 100 mg/kg) prevented this impairment ($p = 0.031$, $p = 0.037$ and $p = 0.032$, respectively). All doses tested were not different when comparing the three chrysin doses (10, 30, and 100 mg/kg) between them ($p > 0.05$).

3.2.2 Biochemical assays

3.2.2.1 ChEs activity

The brain cortex and hippocampus AChE activities are presented in Fig. 8A. Statistical analysis of the brain cortex AChE activity showed no significant difference among the groups ($p = 0.8028$). Statistical analysis of the hippocampus AChE activity showed a significant difference among the groups ($p = 0.001$). Post-hoc comparisons revealed that $AlCl_3$ increased (~38%) the brain cortex AChE activity when compared to the Control group. All doses of chrysin showed a similar significant ability to normalize the AChE activity.

The brain cortex and hippocampus BChE activities are presented in Fig. 8B. Statistical analysis of the brain cortex BChE activity showed no significant difference among the groups ($p = 0.1166$). Statistical analysis of the hippocampus BChE activity showed a significant difference among the groups ($p = 0.001$). Post-hoc comparisons revealed that $AlCl_3$ increased (~31%) the brain cortex AChE activity when compared to the control group. All doses of chrysin showed a similar significant ability to normalize the BChE activity.

3.2.2.2 LPO levels

The brain cortex and hippocampus LPO levels are presented in Fig. 9A. Statistical analysis of the brain cortex LPO levels showed a significant difference among the groups ($p = 0.002$). Post-hoc comparisons revealed that $AlCl_3$ increased (~97%) the brain cortex LPO levels when compared to the control group. Chrysin treatment at all tested doses prevented this increase. Statistical analysis of the hippocampus LPO levels showed a significant difference among the groups ($p = 0.0001$). Post-hoc comparisons revealed that $AlCl_3$ increased (~48%) the hippocampus LPO levels when compared to the control group. All doses of chrysin showed a similar significant antioxidant activity.

3.2.2.3 CP levels

The brain cortex and hippocampus CP levels are presented in Fig. 9B. Statistical analysis of the brain cortex CP levels showed a significant difference among the groups ($p = 0.0167$). Post-hoc comparisons revealed that $AlCl_3$ increased ($\sim 31\%$) the brain cortex CP levels when compared to the control group. Chrysin treatment could not prevent this increase in the brain cortex. Statistical analysis of the hippocampus CP levels showed a significant difference among the groups ($p = 0.004$). Post-hoc comparisons revealed that $AlCl_3$ increased ($\sim 36\%$) the hippocampus CP levels when compared to the control group. All doses of chrysin showed a similar significant antioxidant activity.

3.2.2.4 SOD activity

The brain cortex and hippocampus SOD activities are presented in Fig. 9C. Statistical analysis of the brain cortex SOD activity showed a significant difference among the groups ($p = 0.0001$). Post-hoc comparisons revealed that $AlCl_3$ increased ($\sim 70\%$) the brain cortex SOD activity when compared to the control group. Chrysin treatment in all tested doses prevented this increase. Statistical analysis of the hippocampus SOD activity showed a significant difference among the groups ($p = 0.0001$). Post-hoc comparisons revealed that $AlCl_3$ inhibited ($\sim 28\%$) the hippocampus SOD activity when compared to the control group. All doses of chrysin showed a similar significant ability to normalize the SOD activity.

3.2.2.5 CAT activity

The brain cortex and hippocampus CAT activities are presented in Fig. 9D. Statistical analysis of the brain cortex CAT activity showed no significant difference among the groups ($p = 0.2743$). Statistical analysis of the hippocampus CAT activity showed a significant difference among the groups ($p = 0.0001$). Post-hoc comparisons revealed that $AlCl_3$ inhibited

(~30%) the hippocampus CAT activity when compared to the control group. All doses of chrysin showed a similar significant ability to normalize the CAT activity.

3.2.3 Histopathology and morphometric analysis

Histopathological analysis showed that AlCl_3 exposure induced tissue damage to the cerebral cortex and the hippocampus, causing an increased incidence of degenerating neurons. All groups exposed to AlCl_3 showed some neurons with nuclear disintegration and atrophic cytoplasm. These neurons stained intensely in pink using the hematoxylin method (data not shown), or in dark purple using the thionine acetate method, a pattern that is compatible with eosinophilic neuronal death. As reported in Fig. 10A, morphologically, all chrysin treatments decreased the occurrence of degenerative neurons with necrosis phenotype. The frequency (%) of the necrotic cell in the brain cortex and CA1 hippocampus are presented in Fig. 10B. Quantitative analysis of the brain cortex indicated that treatment with chrysin caused a significant reduction in the frequency of necrotic neurons, especially in the chrysin 100 group. Similar results were observed in the CA1 hippocampus, where all groups treated with chrysin had a lower frequency of necrotic neurons when compared to the AlCl_3 group, being the most significant reduction found in the chrysin 100 group.

4. Discussion

In this study, we showed the ability of chrysin to counteract the early oxidative stress evoked by different oxidant treatments, including H_2O_2 , *t*-BuOOH, and Fenton reaction in presence of AlCl_3 as well as the late neurotoxicity triggered by AlCl_3 in neuronal SH-SY5Y cells. Regarding the antioxidant activity of chrysin, several studies show that the presence of two hydroxyl groups in the chrysin molecule is an important factor determining its antioxidant potency against the oxidation at a cellular level (Huang et al., 2012). Dynamic distribution of

chrysin at a cellular level can contribute to antioxidant effects recorded in neuronal SH-SY5Y cells. A recent *in vitro* study reported a quick uptake or metabolic degradation of chrysin by human hepatocytes after 2 h of incubation in a culture system (Huang et al., 2012). Interestingly, we demonstrated in similar experimental conditions the scavenger activity of chrysin against the ABTS^{•+} radical at membrane levels in neuronal SH-SY5Y cells, suggesting the dynamic distribution of chrysin in the membrane. It was reported the membrane localization and distribution of various flavonoids, including chrysin, can improve the antioxidant activity in proximity to the double bonds of the cell membrane lipids (Günther et al., 2015). These pieces of evidence may underlie the ability of chrysin to reduce the ROS formation elicited by *t*-BuOOH in both neuronal SH-SY5Y and microglial THP-1 cells. Since *t*-BuOOH is an oxidant compound that mimics the LPO in neuronal tissues, these results also suggest the ability of chrysin to counteract the LPO at the neuronal and microglial membrane levels.

The antioxidant activity of chrysin at the membrane level could also modulate the redox signaling in microglial cells. It is noted that NADPH oxidases present in the microglial membrane are a source of ROS, such as H₂O₂ and O₂^{•-}, involved in pro-inflammatory microglial activation (Haslund-Vinding et al., 2017). In this regard, we demonstrated that chrysin reduced both the ROS formation and activation of pro-inflammatory gene expression, such as iNOS, IL-1 β , and TNF α , stimulated by LPS in microglial THP-1 cells, suggesting its potential ability to modulate the redox signaling at the membrane level. These findings corroborate with the ability of chrysin to counteract the oxidative stress-driven neuroinflammation in various experimental models of focal cerebral ischemia/reperfusion injury, Parkinson's disease and isoniazid-induced neurotoxicity (Yao et al., 2014; Goes et al., 2018; Çelik et al., 2020). However, we cannot exclude that chrysin exerts anti-inflammatory effects through other molecular mechanisms such as the inhibition of nuclear factor-kappa B, which is a signaling molecule involved in neuroinflammation (Ha et al., 2010; Li et al., 2019).

1 In this regard, further studies are needed to elucidate the anti-inflammatory mechanisms of
2 chrysin.
3

4
5 Lastly, we demonstrated for the first time the antioxidant activity of chrysin against the
6
7 pro-oxidant ability of Al in neuronal SH-SY5Y cells. The oxidative damage of Al observed in
8
9 various *in vitro* and *in vivo* studies is a feature not expected for a metal without a redox
10
11 capability (Singla and Dhawan, 2013). Several studies suggest that the increase of $O_2^{\cdot-}$ - lifetime
12
13 mediated by Al - $O_2^{\cdot-}$ - complex coupled to Fenton reaction gives oxidative stress in biological
14
15 environments (Singla and Dhawan, 2013). In this context, a recent study demonstrated that
16
17 chrysin has a good scavenging ability for $O_2^{\cdot-}$. This is due to the nucleophilic reaction taking
18
19 place between the unsaturated carbonyl group of chrysin and $O_2^{\cdot-}$ - as well as the single-electron
20
21 transfer between the phenolic hydroxyl group and $O_2^{\cdot-}$ (Zheng et al., 2005). We can therefore
22
23 assume that chrysin breaks the pro-oxidant activity of Al through its ability to neutralize the
24
25 $O_2^{\cdot-}$ - downstream of the oxidative process triggered by Al.
26
27
28
29
30

31
32 The cell membrane is an important biological target of Al^{3+} , and the damage caused to
33
34 membrane components may impair important functions. In particular, Al^{3+} ions altered the lipid
35
36 profile and fluidity of the neuronal membrane, leading to a loss of membrane integrity (Singla
37
38 and Dhawan, 2013). According to these evidence, we recorded the membrane integrity loss in
39
40 terms of necrosis in neuronal SH-SY5Y cells treated with $AlCl_3$ for 24 h. Remarkably, chrysin
41
42 also counteracted the necrosis induced by $AlCl_3$ in neuronal SH-SY5Y cells suggesting its
43
44 ability to preserve the neuronal membrane integrity.
45
46
47

48
49 Taken together, *in vitro* results suggest that antioxidant and neuroprotective effects of
50
51 chrysin against the toxicity of $AlCl_3$ share the same neuronal membrane target. The chrysin
52
53 may act as a membrane shield against early oxidative events that contribute to progressive
54
55 neurodegeneration and neuronal death triggered by $AlCl_3$ exposure.
56
57
58
59
60
61
62
63
64
65

1
2
3
4
5
6
7
8
9
10
11
12
13
14
15
16
17
18
19
20
21
22
23
24
25
26
27
28
29
30
31
32
33
34
35
36
37
38
39
40
41
42
43
44
45
46
47
48
49
50
51
52
53
54
55
56
57
58
59
60
61
62
63
64
65

Considering the limitations of the *in vitro* models to predict the *in vivo* response, the ability of chrysin to counteract the oxidative stress and neuronal death induced by Al was further evaluated in a mouse model of neurotoxicity induced by chronic exposure of ninety days to AlCl₃. Taken together, the *in vivo* results indicate that daily oral chrysin administration during forty-five consecutive days prevented non-spatial learning and memory impairment elicited by AlCl₃. In addition, the chrysin supplementation also normalized the increased activities of AChE and BChE, decreased the oxidative damage, in terms of LPO and protein carbonylation, as well as cell necrosis in the brain cortex and hippocampus.

It is well-known that in neurodegenerative disorders the CNS sensory and motor regions damage can be present (Albers et al., 2015). This kind of impairment can induce false results when behavioral memory tests are assessed. We, therefore, evaluated the motor activity of animals. The OFT and CT performance showed that AlCl₃ treatment did not affect their motor activity and interference in behavioral tests as well as the SDPAT acquisition phase. However, AlCl₃ affected the non-spatial long-term memory as recorded by the latency time decrease in the step down during the retention phase. This cognitive impairment in long-term memory was then recovered by chrysin treatment. In this context, AlCl₃ increased the AChE activity in the hippocampus, but not in the brain cortex, interfering with the processes of memory consolidation as observed in SDPAT. These findings suggest that the impairment of AChE activity in hippocampus structure elicited by AlCl₃ is enough to establish a cognitive deficit. A similar ChE activity pattern in the brain cortex and hippocampus after the different treatments were also recorded for BChE.

Several pre-clinical studies recorded flavonoid-inhibitor effects on ChEs activity indicating their potential use for the treatment of motor neuron and dementia disorders, such as myasthenia gravis, Lewy body dementia, and Alzheimer's disease (Khan et al., 2018). Among the plant-derived flavonoids, chrysin showed the ability to inhibit electric eels' AChE

activity as well as human AChE and BChE in *in vitro* systems (Balkis et al., 2015; Taslimi et al., 2017).

It is established that Al promotes ROS and LPO in different tissues, including the brain (Samarghandian et al., 2019). As expected, the AlCl₃ chronic administration to mice induced a significant LPO, in terms of TBARS levels, in the brain cortex and hippocampus. Remarkably, the chrysin treatment decreased the LPO elicited by AlCl₃ in both brain regions confirming its ability to protect the tissue membrane from oxidative damage. These *in vivo* results corroborate with the *in vitro* antioxidant profile of chrysin recorded in neuronal SH-SY5Y cells.

Along with the LPO elevation, the ROS formation also causes protein oxidation with the formation of various carbonyl species. In this regard, AlCl₃ chronic exposure increased the CP levels in the brain cortex and hippocampus, indicating that the pro-oxidant action of Al targets both the polyunsaturated fatty acids and proteins. Remarkably, the chrysin treatment decreased the CP levels suggesting the ability of this flavonoid to prevent the triggering of the protein carbonylation process. It is noted that the protein carbonylation is non-enzymatic leading to irreversible modifications in proteins (Ferdorova et al., 2014).

The role and effectiveness of the first-line defense antioxidants that include SOD, CAT, and glutathione peroxidase (GPX) are important and indispensable in the entire defense strategy of antioxidants, including flavonoids (Ighodaro and Akinloye, 2017). Under oxidative stress conditions, SOD acts as a first-line defense against superoxide as it converts the O₂^{•-} radical to H₂O₂ and molecular oxygen. Then CAT and the GPX, using reduced glutathione, converts the H₂O₂ into H₂O (Maya et al., 2016). Considering that, Al can strengthen the oxidative capacity of O₂^{•-}, directly or indirectly through catalysis of the Fenton reaction, we, therefore, assessed the activity of SOD and CAT, two enzymes involved in the first extremely efficient reactions of O₂^{•-} detoxification.

The conflicting effects promoted by Al on CAT and SOD activities in different rodent brain regions has been described in the literature (Atienzar et al., 1998; Yuan et al., 2012; Jelenković et al., 2014; Benyettou et al., 2017; Sadauskiene et al., 2020), highlighting critical experimental conditions, such as Al concentration, treatment time, species and age of animals. Our *in vivo* studies showed that the AlCl₃ treatment for 90 days inhibited CAT and SOD activities in the hippocampus and increased the SOD activity in the cortex. The contradictory increase of SOD can be interpreted as an adaptive neuronal response of the frontal cortex involving a strong oxidative stress increase elicited by Al (Navarro et al., 2009). The different composition of lipids between brain cortex and hippocampus and cortex could explain a greater O₂^{•-} formation induced by Al and antioxidant response in terms of SOD levels in the hippocampus. However, the chrysin treatment was able to reverse these enzymes activities alterations, corroborating with the ability of chrysin to counteract early oxidant events at a brain level.

Chronic oxidative damage induced by Al also leads to neuronal death, predominant in necrosis (Feng et al., 2014; Yamawaki et al., 2019). The neuronal death in the brain cortex and hippocampus can affect the learning and memory processes (Matthews, 2015; Yamawaki et al., 2019). Our histological results in mice recorded that the treatment with AlCl₃ induces significant neurodegeneration in the brain cortex and hippocampus. In particular, the histological analysis showed focal and neurodegenerative changes along with the increased number of degenerative neurons with necrosis phenotype. In this regard, the necrotic neuron frequency in the brain cortex was higher than hippocampus suggesting that the cortex is the most sensitive brain area to neuronal damage elicited by AlCl₃. Interestingly, a recent study recorded that the Al content of different human brain tissues, including cortex, in AD, autism spectrum disorder, and multiple sclerosis was significantly elevated suggesting a critical role of this metal in the etiology of these neurodegenerative diseases (Exley and Mold, 2019). The

neurodegeneration in terms of necrosis was attenuated by chrysin in both the brain cortex and hippocampus.

Taken together, *in vivo* results show that oral administration of chrysin can prevent and counteract oxidative damage and neurodegeneration in the brain cortex and hippocampus prompted by chronic exposure to AlCl_3 . In particular, all the doses (10, 30, and 100 mg/kg) of chrysin used showed significant antioxidant and neuroprotective effects in both brain regions. However, the dose of 10 mg/kg chrysin already exhibited the maximum antioxidant and neuroprotective activity at a brain level. This evidence suggests that the BBB crossing processes could become saturated limiting the increase of the chrysin levels in the brain. After oral administration, the chrysin is highly biotransformed in the liver, during which conjugated metabolites chrysin-7-sulfate and chrysin-7-glucuronide are formed in mice (Mohos et al., 2020). Despite these conjugates appear at higher concentrations in the circulation than chrysin, they probably do not contribute to the cerebral effects because they cannot cross the BBB as predicted by *in silico* studies (Daiana and Zoete, 2016; Daiana et al., 2016). These evidence, therefore, support that chrysin is predominant in brain action. It is probably that rising the dose of chrysin also increases its metabolites that limit the availability of chrysin in the circulation to cross the BBB, explaining the same neuroprotective effects recorded between 10 and 100 mg/kg.

5. Conclusion

This study demonstrates the ability of chrysin by oral administration to protect critical brain regions for cognitive function from oxidative damage and neurodegeneration induced by chronic AlCl_3 exposure. Regarding the mechanisms of neuroprotective action, chrysin showed the ability to act as a membrane shield against early oxidative events mediated by $\text{O}_2^{\cdot-}$ and other ROS that contribute to neuronal death triggered by AlCl_3 exposure.

1 These findings support the potential use of chrysin as a food supplement for the
2 prevention of neurological and neurodegenerative diseases or the maintenance of a healthy
3 brain.
4
5
6
7
8
9

10 **Conflict of interest**

11 The authors disclose no actual or potential conflicts of interest, including financial,
12 personal, or relationships with other people or organizations. All authors have contributed to
13 the work and agreed with the presented findings.
14
15
16
17
18
19
20
21

22 **Acknowledgments**

23 This work was supported by Coordenação de Aperfeiçoamento de Pessoal de Nível
24 Superior (CAPES), Conselho Nacional de Desenvolvimento Científico e Tecnológico (CNPq)
25 and Fundação de Amparo à Pesquisa do Estado de Goiás (FAPEG).
26
27
28
29
30
31
32
33

34 **6. References**

- 35
36 Aebi, H., 1984. Catalase. Enzyme Act Oxidoreductases. 51, 674–684.
37
38 <https://doi.org/10.1086/330448>.
39
40
41 Albers, M.W., Gilmore, G.C., Kaye, J., Murphy, C., Wingfield, A., Bennett, D.A., Boxer, A.L.,
42
43 Buchman, A.S., Cruickshanks, K.J., et al. 2015. At the interface of sensory and motor
44 dysfunctions and Alzheimer's disease. *Alzheimers Dement.* 11, 70–98.
45
46 <https://doi.org/10.1016/j.jalz.2014.04.514>.
47
48
49
50
51 Atienzar, F., Desor, D., Burnel, D., Keller, J. M., Lehr, P., Vasseur, P., 1998. Effect of
52 aluminum on superoxide dismutase activity in the adult rat brain. *Biological Trace*
53
54
55
56
57
58
59
60
61
62
63
64
65

- Balkis, A., Tran, K., Lee, Y.Z., Ng, K., 2015. Screening flavonoids for inhibition of acetylcholinesterase identified baicalein as the most potent inhibitor. *The Journal of Agricultural Science*. 7, 26–35. <https://doi.org/10.5539/jas.v7n9p26>.
- Benyettou, I., Kharoubi, O., Hallal, N., Benyettou H.A., Tair, K., Belmokhtar, M., Aoues, A., Ozaslan, M., 2017. Aluminium-induced behavioral changes and oxidative stress in developing rat brain and the possible ameliorating role of omega-6/omega-3 ratio. *Journal of Biological Sciences*. 17, 106-117. <https://doi.org/10.3923/jbs.2017.106.117>.
- Boissier, J., Tardy, J., Diverres, J.C., 1960. Une nouvelle méthode simple pour explorer l'action «tranquillisante»: le test de la cheminée. *Journal of Experimental Medicine*. 3, 81–84. <https://doi.org/10.1159/000134913>.
- Borowska S, Brzóska MM., 2015. Metals in cosmetics: implications for human health. *Journal of Applied Toxicology*. 35(6), 551-72. <https://doi.org/10.1002/jat.3129>.
- Bradford, M.M., 1976. A rapid and sensitive method for the quantitation of microgram quantities of protein utilizing the principle of protein-dye binding. *Analytical Biochemistry*. 72, 248–254. [https://doi.org/10.1016/0003-2697\(76\)90527-3](https://doi.org/10.1016/0003-2697(76)90527-3).
- Çelik, H., Kucukler, S., Çomaklı, S., Caglayan, C., Özdemir, S., Yardım, A., Karaman, M., Kandemir, F.M., 2020. Neuroprotective effect of chrysin on isoniazid-induced neurotoxicity via suppression of oxidative stress, inflammation and apoptosis in rats. *Neurotoxicology*. 81, 197-208. <https://doi.org/10.1016/j.neuro.2020.10.009>.
- Christine, W., Dagmar, F., Berenike, L., Christian, T., Teodora, N., John, B., Peter, G., Peter, W., Anna, S.S., Stefan, K., Cornelia, D., 2018. T-BuOOH induces ferroptosis in human and murine cell lines. *Archives of Toxicology*. 92, 759–775. <https://doi.org/10.1007/s00204-017-2066-y>.

- Daiana, A., and Zoete, V., 2016. A boiled- egg to predict gastrointestinal absorption and brain penetration of small molecules. *Chemistry Europe*. 11, 1117–1121. <https://doi.org/10.1002/cmdc.201600182>. Available: <http://www.swissadme.ch/>.
- Daiana, A., Michielin, O., Zoete, V., 2016. SwissADME: a free web tool to evaluate pharmacokinetics, drug-likeness and medicinal chemistry friendliness of small molecules. *Scientific reports*. 7:42717, 1–12. <https://doi.org/10.1038/srep42717>. Available: <http://www.swissadme.ch/>.
- Di Martino, R.M.C., Pruccoli, L., Bisi, A., Gobbi, S., Rampa, A., Martinez, A., Pérez C., Martinez-Gonzalez, L., Paglione, M., Di Schiavi, E., Seghetti, F., Tarozzi, A., Belluti, F., 2020. Novel curcumin-diethyl fumarate hybrid as a dualistic gsk-3 β inhibitor/nrf2 inducer for the treatment of Parkinson's disease. *ACS Chemical Neuroscience*. 2020, 1-30. <https://doi.org/10.1021/acscemneuro.0c00363>.
- Drobyshev, E. J., Solovyev, N. D., Gorokhovskiy, B.M., Kashuro, V. A., 2018. Accumulation patterns of sub-chronic aluminum toxicity model after gastrointestinal administration in rats. *Biological Trace Element Research*. 185, 384–394. <https://doi.org/10.1007/s12011-018-1247-8>.
- El-Askarya, H., Haggagb, M., Husseina, D., Husseinb, S., Sleemd, A., 2017. Bioactivity-guided study of *Passiflora caerulea* L. leaf extracts. *Iranian Journal of Pharmaceutical Research*. 16, 46–57. PMID:29844775.
- Ellman, G.L., Courtney, K.D., Andres, V., Feather-Stone, R.M., 1961. A new and rapid colorimetric determination of acetylcholinesterase activity. *Biochemical Pharmacology*. 7, 88–95. [https://doi.org/10.1016/0006-2952\(61\)90145-9](https://doi.org/10.1016/0006-2952(61)90145-9).
- Exley, C., 2013. Human exposure to aluminium. *Environmental Science: Processes & Impacts*. 15, 1785–1970. <https://doi.org/10.1039/c3em00374d>.

- 1 Farhat, S.M., Mahboob, A., Ahmed, P., 2019. Oral exposure to aluminum leads to reduced
2 nicotinic acetylcholine receptor gene expression, severe neurodegeneration and impaired
3 hippocampus dependent learning in mice. *Drug and Chemical Toxicology*. 54, 1–9.
4
5 [https://doi.org/ 10.1080/01480545.2019.1587452](https://doi.org/10.1080/01480545.2019.1587452).
6
7
8
9 Farkhondeh, T., Abedi, F., Samarghandian, S., 2019. Chrysin attenuates inflammatory and
10 metabolic disorder indices in aged male rat. *Biomedicine & Pharmacotherapy*. 109,
11 1120–1125. <https://doi.org/10.1016/j.biopha.2018.10.059>.
12
13
14
15
16 Fedorova, M., Bollineni, R.C., Hffmann, R., 2014. Protein carbonylation as a major hallmark
17 of oxidative damage: update of analytical strategies. *Mass Spectrometry Reviews*. 33,
18 79–97. [https://doi.org/ 10.1002/mas.21381](https://doi.org/10.1002/mas.21381).
19
20
21
22
23 Feng, X., Qin, H., Shi, Q., Zhang, Y., Zhou, F., Wu, H., Ding, S., Niu, Z., Shen, P., 2014.
24 Chrysin attenuates inflammation by regulating M1/M2 status via activating PPAR γ .
25
26 *Biochemical Pharmacology*. 89, 503–514. <https://doi.org/10.1016/j.bcp.2014.03.016>.
27
28
29
30
31
32
33
34
35
36
37
38
39
40
41
42
43
44
45
46
47
48
49
50
51
52
53
54
55
56
57
58
59
60
61
62
63
64
65
- Garza-Lombó, C., Posadas, Y., Quintanar, L., Gonsebatt, M.E., Franco, R., 2018.
Neurotoxicity linked to dysfunctional metal ion homeostasis and xenobiotic metal
exposure: redox signaling and oxidative stress. *Antioxidants & Redox Signaling*. 28(18),
1669-1703. <https://doi.org/10.1089/ars.2017.7272>.
Goes, A.T., Jesse, C.R., Antunes, M.S., Lobo, F.V, Lobo, A.B., Luchese, C., Paroul, N., Boeira,
S.P., 2018. Protective role of chrysin on 6-hydroxydopamine-induced neurodegeneration
a mouse model of Parkinson's disease: Involvement of neuroinflammation and

- neurotrophins. Chemical-Biological Interactions. 5:279, 111-120.
<https://doi.org/10.1016/j.cbi.2017.10.019>.
- Günther, G., Berríos, E., Pizarro, N., Valdés, K., Montero, G., Arriagada, F., Morales, J., 2015. Flavonoids in microheterogeneous media, relationship between their relative location and their reactivity towards singlet oxygen. *Plus One*. 10, 729-749. <https://doi.org/10.1371/journal.pone.0129749>.
- Ha, S.K., Moon, E., Kim, S.Y., 2010. Chrysin suppresses LPS-stimulated proinflammatory responses by blocking NF- κ B and JNK activations in microglia cells. *Neuroscience Letters*. 26:485, 143-147. <https://doi.org/10.1016/j.neulet.2010.08.064>.
- Hadjmohammadi, Saman, S., M., Nazari, J., 2010. Separation optimization of quercetin, hesperetin and chrysin in honey by micellar liquid chromatography and experimental design. *Journal of Separation Science*. 33, 3144–3151. <https://doi.org/10.1002/jssc.201000326>.
- Haslund-Vinding, J., McBean, G., Jaquet, V., Vilhardt, F., 2017. NADPH oxidases in oxidant production by microglia: activating receptors, pharmacology and association with disease. *British Journal of Pharmacology*. 174(12), 1733-1749. <https://doi.org/10.1111/bph.13425>.
- He, X., Wang, Y., Bi, M., Du, G., 2012. Chrysin improves cognitive deficits and brain damage induced by chronic cerebral hypoperfusion in rats. *British Journal of Pharmacology*. 680, 41–48. <https://doi.org/10.1016/j.ejphar.2012.01.025>.
- Huang, C.S., Lii, C.K., Lin, A.H., Yeh, Y.W., Yao, H.T., Li, C.C., Wang, T.S., Chen, H.W., 2012. Protection by chrysin, apigenin, and luteolin against oxidative stress is mediated by the Nrf2-dependent up-regulation of heme oxygenase 1 and glutamate cysteine ligase in rat primary hepatocytes. *Archives of Toxicology*. 87(1), 167-178. <https://doi.org/10.1007/s00204-012-0913-4>.

- Ighodaro, O.M., Akinloye, O.A., 2017. First line defence antioxidants-superoxide dismutase (SOD), catalase (CAT) and glutathione peroxidase (GPX): Their fundamental role in the entire antioxidant defence grid. *Alexandria Journal of Medicine*. 2017, 1-7. <https://doi.org/10.1016/j.ajme.2017.09.001> 209.
- Jelenković, A, Jovanović MD, Stevanović I, Petronijević N, Bokonjić D, Zivković J, Igić R., 2014. Influence of the green tea leaf extract on neurotoxicity of aluminium chloride in rats. *Phytotherapy Research*. 28(1):82-87. <https://doi.org/10.1002/ptr.4962>.
- Kalogeropoulos, N., Yanni, A., Koutrotsios, G., Aloup, M., 2013. Bioactive microconstituents and antioxidant properties of wild edible mushrooms from the island of Lesbos, Greece. 55, 378–385. <https://doi.org/10.1016/j.fct.2013.01.010>.
- Kameyama, T., Nabeshima, T., Kozawa, T., 1986. Step-down-type passive avoidance- and escape-learning method - Suitability for experimental amnesia models. *Journal of Pharmacological and Toxicological Methods*. 16, 39–52. [https://doi.org/10.1016/0160-5402\(86\)90027-6](https://doi.org/10.1016/0160-5402(86)90027-6).
- Khan, H., Marya, S., Amin, M.A., Kamal, S., Patel, S., 2018. Flavonoids as acetylcholinesterase inhibitors: Current therapeutic standing and future prospects. *Biomedicine & Pharmacotherapy*. 101, 860–870. <https://doi.org/10.1016/j.biopha.2018.03.007>.
- Klotz K, Weistenhöfer W, Neff F, Hartwig A, van Thriel C, Drexler H., 2017. The Health Effects of Aluminum Exposure. *Deutsches Ärzteblatt International* 114(39), 653-659. <https://doi.org/10.3238/arztebl.2017.0653>.
- Krewski, D., Yokel, R., Nieboer, E., Borchelt, D., Cohen, J., Harry, J., Kacew, S., Lindsay, J., Mahfouz, A., Rondeau, V., 2007. Human health risk assessment for aluminium, aluminium oxide, and aluminium hydroxide. *Journal of Toxicology and Environmental Health*. 10, 1–269. <https://doi.org/10.1080/10937400701597766>.

- Levine, R.L., Garland, D., Oliver, C.N., Amici, A., Climent, I., Lenz, A.G., Ahn, S., Shaltiel, E.R., 1990. Determination of carbonyl content in oxidatively modified proteins. *Methods in Enzymology*. 186, 464–478. [https://doi.org/10.1016/0076-6879\(90\)86141-H](https://doi.org/10.1016/0076-6879(90)86141-H).
- Li, R., Zang, A., Zhang, L., Zhang, H., Zhao, L., Qi, Z., Wang, H., 2014. Chrysin ameliorates diabetes-associated cognitive deficits in Wistar rats. *Neurological Sciences*. 35, 1527–1532. <https://doi.org/10.1007/s10072-014-1784-7>.
- Li, Z., Chu, S., He, W., Zhang, Z., Liu, J., Cui, L., Yan, X., Li, D., Chen, N., 2019. A20 as a novel target for the anti-neuroinflammatory effect of chrysin via inhibition of NF- κ B signaling pathway. *Brain, Behavior, and Immunity*. 79, 228-235. <https://doi.org/10.1016/j.bbi.2019.02.005>.
- Lukiw, W.J., Kruck, T.P.A., Percy, M.E., Pogue A.I., Alexandrov, P.N. Walsh, W.J, Sharfman N.M., Jaber, V.R., Zhao, Y., Li, W., Bergeron, C., Culicchia, F., Fang, Z., McLachlan, D.R.C., 2018. Aluminum in neurological disease - a 36-year multicenter study. *Journal of Alzheimers Disease and Parkinsonism*. 8, 457–469. <https://doi.org/10.4172/2161-0460.1000457>.
- Mani, R., and Natesan, V., 2018. Chrysin: Sources, beneficial pharmacological activities, and molecular mechanism of action. *Phytochemistry*. 145, 187–196. <https://doi.org/10.1016/j.phytochem.2017.09.016>.
- Manzoli, E.S., Serpeloni, J.M., Grotto, D., Bastos, J.K., Antunes, L.M., Barbosa, J.F., Barcelos, G.R., 2015. Protective effects of the flavonoid chrysin against methylmercury-induced genotoxicity and alterations of antioxidant status, in vivo. *Oxidative Medicine and Cellular Longevity*. 2015, 1-8. <https://doi.org/10.1155/2015/602360>.
- Matthews, B.R., 2015. Memory dysfunction. *Behavioral Neurology and Neuropsychology*. 21, 613–626. <https://doi.org/10.1212/01.CON.0000466656.59413.29>.

- Maya S., Prakash, T., Madhu, K.D., Goli D., 2016. Multifaceted effects of aluminium in neurodegenerative diseases: A review. *Biomedicine & Pharmacotherapy*. 83, 746-754. <https://doi.org/10.1016/j.biopha.2016.07.035>.
- Misra, H.P., Fridovich, I., 1972. The role of superoxide anion in the autoxidation of epinephrine and a simple assay for superoxide dismutase. *Journal of Biological Chemistry*. 247(10):3170-5. PMID: 4623845
- Mohos, V., Fliszár-Nyúl, E., Schilli, G., Hetényi, C., Lemli, B., Kunsági-Máté, S., Bognár B., Poór, M., 2018. Interaction of Chrysin and Its Main Conjugated Metabolites Chrysin-7-Sulfate and Chrysin-7-Glucuronide with Serum Albumin. *International Journal of Molecular Sciences*. 19, 1-15. <https://doi.org/10.3390/ijms19124073>.
- Mohos, V., Fliszár-Nyúl, E., Ungvári, O., Bakos, É., Kuffa, K., Bencsik, T., Zsidó, B.Z., Hetényi, C., Telbisz, Á., Özvegy-Laczka, C., Poór, M., 2020. Effects of chrysin and its major conjugated metabolites chrysin-7-sulfate and chrysin-7-glucuronide on cytochrome p450 enzymes and on OATP, P-gp, BCRP, and MRP2 transporters. *Drug Metabolism & Disposition*. 48(10), 1064-1073. <https://doi.org/10.1124/dmd.120.000085>.
- Montgomery, K.C., 1955. The relation between fear induced by novel stimulation and exploratory behavior. *Journal of Comparative Psychology*. 254–260. <https://doi.org/10.1037//0033-2909.126.1.78>.
- Nabavi, F.S., Braid, N., Habtemariam, S., Erdogan, I., Daglia, M., Manayi, A., Gortzi, O., Nabavi, S.M., 2015. Neuroprotective effects of chrysin: From chemistry to medicine. *Neurochemistry International*. 90, 224–231. <https://doi.org/10.1016/j.neuint.2015.09.006>.
- Navarro A, Boveris A, Báñez M., Sánchez-Pino M., Gómez C, Muntané G, Ferrer I., 2009. Human brain cortex: mitochondrial oxidative damage and adaptive response in Parkinson

- disease and in dementia with Lewy bodies. *Free Radical Biology & Medicine*. 46(12):1574-1580. <https://doi.org/10.1016/j.freeradbiomed.2009.03.007>.
- Ohkawa, H., Ohishi, N., Yagi, K., 1979. Assay for lipid peroxides in animal tissues by thiobarbituric acid reaction. *Analytical Biochemistry*. 95, 351–358. [https://doi.org/10.1016/0003-2697\(79\)90738-3](https://doi.org/10.1016/0003-2697(79)90738-3).
- Oliveira, T.S., Thomaz, D.V., da Silva, H.F., Cerqueira, L.B., Garcia, L.F., Gil, H.P.V., Pontarolo, R., Campos, F.R., Costa, E.A., Santos, F.C.S., Gil, E.S., Ghedini, P.C., 2018. Neuroprotective effect of *Caryocar brasiliense* camb. Leaves is associated with anticholinesterase and antioxidant properties. *Oxidative Medicine and Cellular Longevity*. 1–12. <https://doi.org/10.1155/2018/9842908>.
- Ortiz, C.J.C., Damasio, C.M., Pruccoli, L., Nadur, N.F., de Azevedo, L.L., Guedes, I.A., Dardenne, L.E., Kümmerle, A.E., Tarozzi, A., Viegas, C. J., 2020. Cinnamoyl-n-acylhydrazone-donepezil hybrids: synthesis and evaluation of novel multifunctional ligands against neurodegenerative diseases. *Neurochemical Research*. 45, 3003–3020. <https://doi.org/10.1007/s11064-020-03148-2>.
- Pruccoli, L., Morroni, F., Sita, G., Hrelia, P., Tarozzi, A., 2020. Esculetin as a bifunctional antioxidant prevents and counteracts the oxidative stress and neuronal death induced by amyloid protein in SH-SY5Y cells. *Antioxidants*. 9(6), 551-566. <https://doi.org/10.3390/antiox9060551>.
- Reis, J.S., Oliveira, G.B., Monteiro, M.C., Machado, C.S., Torres, Y.R., Prediger, R.D., Maia, C.S., 2014. Antidepressant- and anxiolytic-like activities of an oil extract of propolis in rats. *Phytomedicine*. 21, 1466–1472. <https://doi.org/10.1016/j.phymed.2014.06.001>.
- Ruipérez, F., Mujika, J.I., Ugalde, J.M., Exley, C., Lopez, X., 2012. Pro-oxidant activity of aluminum: promoting the Fenton reaction by reducing Fe(III) to Fe(II). *Journal of Inorganic Biochemistry*. 117, 118-123. <https://doi.org/10.1016/j.jinorgbio.2012.09.008>.

- Sadauskiene, I., Liekis, A., Staneviciene, I., Naginiene, R., Ivanov, L., 2020. Effects of long-term supplementation with aluminum or selenium on the activities of antioxidant enzymes in mouse brain and liver. *Catalysts*. 10(5), 585. <https://doi.org/10.3390/catal10050585>.
- Sairazi, N.S.M., Sirajudeen, K.N.S., Asari, M.A., Mummedy, S., Muzaimi, M., Sulaiman, S.A. 2017. Effect of tualang honey against KA-induced oxidative stress and neurodegeneration in the cortex of rats. *BMC Complementary Medicine and Therapies*. 17–31. <https://doi.org/10.1186/s12906-016-1534-x>.
- Samarghandian, S., Farkhondeh, T., Azimi-nezhad, M., Mohammad, A., Shahri. P., 2019. Antidotal or protective effects of honey and chrysin, its major polyphenols, against natural and chemical toxicities. *Acta Biomedica*. 90, 2–18. <https://doi.org/10.23750/abm.v90i4.7534>.
- Sarkaki, A., Farbood, Y., Mansouri, S.M.T., Badavi, M., Khorsandi, L., Dehcheshmeh, M.G., Shooshtari, M.K., 2019. Chrysin prevents cognitive and hippocampal long-term potentiation deficits and inflammation in rat with cerebral hypoperfusion and reperfusion injury. *Life Science*. 226, 2002–209. <https://doi.org/10.1016/j.lfs.2019.04.027>.
- Singla, N., Dhawan, D.K., 2013. Zinc protection against aluminium induced altered lipid profile and membrane integrity. *Food and Chemical Toxicology*. 55, 18-28. <https://doi.org/10.1016/j.fct.2012.12.047>. Epub 2013 Jan 9. PMID: 23313339.
- Tal, Y., Anavi, S., Reisman, M., Samach, A., Tirosh, O., Troen, A.M., 2016. The neuroprotective properties of a novel variety of passion fruit. *Journal of Functional Foods*. 23, 359–369. <https://doi.org/10.1016/j.jff.2016.02.039>.
- Tarozzi, A., Bartolini, M., Piazzzi, L., Valgimigli, L., Amorati, R., Bolondi, C., Djemil, A., Mancini, F., Andrisano, V., Rampa, A., 2014. From the dual function lead AP2238 to

- AP2469, a multi-target-directed ligand for the treatment of Alzheimer's disease. Pharmacology Research & Perspectives. 2(2), 1-14. <https://doi.org/10.1002/prp2.23>.
- Tarozzi, A., Morroni, F., Bolondi, C., Sita, G., Hrelia P., Djemil, A., Cantelli-Forti, G., 2012. Neuroprotective effects of erucin against 6-hydroxydopamine-induced oxidative damage in a dopaminergic-like neuroblastoma cell line. International Journal of Molecular Sciences. 13(9), 10899–1091. <https://doi.org/10.3390/ijms130910899>
- Taslimi, P., Caglayan, C., Gulcin, I., 2017. The impact of some natural phenolic compounds on carbonic anhydrase, acetylcholinesterase, butyrylcholinesterase, and α -glycosidase enzymes: An antidiabetic, anticholinergic, and antiepileptic study. Journal of Biochemical and Molecular Toxicology. 31, 1–7. <https://doi.org/10.1002/jbt.21995>.
- Thomaz, D.V., Peixoto, L.F., Oliveira, T.S., Fajemiroye, J.O., Neri, H.F.S., Xavier, C.H., Costa, E.A., Santos, F.C.A., Gil, E.S., Ghedini, P.C., 2018. Antioxidant and neuroprotective properties of *Eugenia dysenterica* leaves. Oxidative Medicine and Cellular Longevity. 2018, 1–10. <https://doi.org/10.1155/2018/3250908>.
- Willhite, C.C., Karyakina, N.A., Yokel, R.A., Yenugadhati, N., Wisniewski, T.M., Arnold, I.M., Momoli, F., Krewski, D., 2014. Systematic review of potential health risks posed by pharmaceutical, occupational and consumer exposures to metallic and nanoscale aluminum, aluminum oxides, aluminum hydroxide and its soluble salts. Critical Reviews in Toxicology. 44, 1–80. <https://doi.org/10.3109/10408444.2014.934439>
- Yamawaki, N., Corcoran, K.A., Guedea, A.L., Shepherd, G.M., Radulovic, G., 2019. Differential contributions of glutamatergic hippocampal - retrosplenial cortical projections to the formation and persistence of context memories. Cerebral Cortex. 29, 2728–2736. <https://doi.org/10.1093/cercor/bhy142>.
- Yao, Y., Chen, L., Xiao, J., Wang, C., Jiang, W., Zhang, R., Hao, J., 2014. Chrysin protects against focal cerebral ischemia/reperfusion injury in mice through attenuation of

oxidative stress and inflammation. International Journal of Molecular Sciences. 13:15,
20913 - 20926. <https://doi.org/10.3390/ijms151120913>.

Yuan CY, Lee YJ, Hsu G.S., 2012. Aluminum overload increases oxidative stress in four
functional brain areas of neonatal rats. Journal of Biomedical Science. 19(1), 30-51.
<https://doi.org/10.1186/1423-0127-19-51>.

Zheng, J.B., Zhang, H.F., Gao, H., 2005. Investigation on electrochemical behavior and
scavenging superoxide anion ability of chrysin at mercury electrode. Chinese Journal of
Chemistry. 23(8), 1042-1046. <https://doi.org/10.1002/cjoc.200591042>.

Figure captions

Figure 1. Chemical structure of chrysin (IUPAC: 5,7-Dihydroxy-2-phenyl-4H-chromen-4-one, CAS registry number: 480-40-0).

Figure 2. Cytotoxicity and antioxidant activity of chrysin against H₂O₂-induced ROS formation in neuronal SH-SY5Y cells. **(A)** Cells were incubated for 24 h with various concentrations of chrysin (1.25 – 40 µM). At the end of incubation, the neuronal viability was measured using MTT assay. **(B)** Cells were incubated for 30 min with the fluorescent probe H₂DCF-DA. At the end of incubation, cells were treated with various concentrations of chrysin (1.25 – 5 µM) and H₂O₂ (100 µM). Data are represented as mean ± SEM of three independent experiments. Statistical analysis was performed using one-way ANOVA followed by Dunnett's test. ^ap = 0.0031, ^bp = 0.0001, and ^cp = 0.0001 when compared to cells treated with H₂O₂.

Figure 3. Antioxidant activity of chrysin against *t*-BuOOH-induced ROS formation in neuronal SH-SY5Y **(A)** and microglial THP-1 cells **(B)**. Cells were incubated for 30 min with the fluorescent probe H₂DCF-DA. At the end of incubation, cells were treated for 30 min with various concentrations of chrysin (1.25 – 5 µM) and *t*-BuOOH (100 µM). Data are represented as mean ± SEM of three independent experiments. Statistical analysis was performed using one-way ANOVA followed by Dunnett's test. **(A)** ^ap = 0.0335, ^bp = 0.0449, and ^cp = 0.0118 when compared to cells treated with *t*-BuOOH; **(B)** ^ap = 0.0035 when compared to cells treated with *t*-BuOOH.

Figure 4. Effects of chrysin against the oxidative stress and inflammation induced by LPS in microglial THP-1 cells. **(A)** Cells were incubated for 24 h with chrysin (5 μ M) and LPS (1 μ g/mL). At the end of incubation, ROS formation was measured using the fluorescent probe H₂DCF-DA. Data are represented as mean \pm SEM of three independent experiments. Statistical analysis was performed using Student's t-test. ^ap = 0.0020 when compared to cells treated with LPS. **(B-D)** Cells were incubated for 24 h with chrysin (5 μ M) and LPS (1 μ g/mL). At the end of incubation, iNOS **(B)**, IL-1 β **(C)** and TNF α **(D)** expression was measured by quantitative RT-PCR. Data are represented as mean \pm SEM of three independent experiments. Statistical analysis was performed using one-way ANOVA followed by Bonferroni's test. **(B)** ^ap = 0.0001 when compared to untreated cells and ^bp = 0.0154 when compared to cells treated with LPS; **(C)** ^ap = 0.0001 when compared to untreated cells and ^bp = 0.0122 when compared to cells treated with LPS; **(D)** ^ap = 0.0001 when compared to untreated cells and ^bp = 0.0038 when compared to cells treated with LPS.

Figure 5. Antioxidant activity of chrysin against the pro-oxidant effect of AlCl₃ on Fenton reaction in neuronal SH-SY5Y cells. Cells were incubated for 30 min with the fluorescent probe H₂DCF-DA. At the end of incubation, cells were first treated for 15 min with FeSO₄/H₂O₂/AlCl₃ (50 μ M, 200 μ M, and 50 μ M, respectively) and then treated for 15 min with chrysin (5 μ M). Data are represented as mean \pm SEM of three independent experiments. Statistical analysis was performed using one-way ANOVA followed by Bonferroni's test. ^ap = 0.0031 when compared to untreated cells, ^bp = 0.0022 when compared to cells treated with FeSO₄/H₂O₂ and ^cp = 0.0012 when compared to cells treated with FeSO₄/H₂O₂/AlCl₃.

Figure 6. Neuroprotective effects of chrysin against the cytotoxicity induced by AlCl₃ in neuronal SH-SY5Y cells. Cells were incubated for 24 h with chrysin (5 μ M) and AlCl₃ (50

1 μM). At the end of incubation, the cytotoxicity of AlCl_3 in terms of cytostatic effect (A) and
2 necrosis (B) was assessed using trypan blue and propidium iodide, respectively. (C)
3
4 Representative bright field (BF) and PI fluorescence images. Scale bars: 100 μM . Data are
5
6 represented as mean \pm SEM of three independent experiments. Statistical analysis was
7
8 performed using one-way ANOVA followed by Bonferroni's test. (A) ^a $p = 0.0033$ when
9
10 compared to untreated cells and ^b $p = 0.0432$ when compared to cells treated with AlCl_3 ; (B) ^a
11
12 $p = 0.0010$ when compared to untreated cells and ^b $p = 0.0071$ when compared to cells treated
13
14 with AlCl_3 .
15
16
17
18
19
20
21

22 **Figure 7.** Effect of chrysin on AlCl_3 induced memory impairment in the step-down passive
23 avoidance task. Data are represented as mean \pm SEM. for $n = 14$ to 16 animals per group.
24
25 Statistical analysis was performed using one-way ANOVA followed by Tukey's test. ^a $p < 0.05$
26
27 when compared to the control group; ^b $p = 0.0310$ when compared to the AlCl_3 group. ^c $p =$
28
29 0.0370 when compared to the AlCl_3 group; ^d $p = 0.0320$ when compared to the AlCl_3 group.
30
31
32
33
34
35

36 **Figure 8.** Effect of chrysin on brain cortex and hippocampus AChE (A) and BChE (B) activities
37 of mice treated with AlCl_3 . Data are represented as mean \pm SEM. for $n = 8$ animals per group.
38
39 Statistical analysis was performed using one-way ANOVA followed by Tukey's test. (A) ^e $p =$
40
41 0.0013 when compared to the control group; ^f $p = 0.0118$, ^g $p = 0.0187$, and ^h $p = 0.0215$ when
42
43 compared to the AlCl_3 group for hippocampus AChE activity; (B) ^e $p < 0.0002$ when compared
44
45 to the control group; ^f $p = 0.111$, ^g $p = 0.0115$, and ^h $p = 0.0194$ when compared to the AlCl_3
46
47 group for hippocampus BChE activity.
48
49
50
51
52
53
54
55

56 **Figure 9.** Effect of chrysin on brain cortex and hippocampus LPO levels (A), CP levels (B),
57
58 SOD activities (C) and CAT activities (D) of mice treated with AlCl_3 . Data are represented as
59
60
61
62
63
64
65

mean \pm SEM. for n = 8 animals per group. Statistical analysis was performed using one-way ANOVA followed by Tukey's test. **(A)** ^a p = 0.0001 when compared to the control group, ^b p = 0.001, ^c p = 0.032, and ^d p = 0.010 when compared to the AlCl₃ group, for brain cortex MDA levels; ^e p = 0.0005 when compared to the control group; ^f p = 0.0002, ^g p = 0.0001, and ^h p = 0.0001 when compared to the AlCl₃ group, for hippocampus MDA levels. **(B)** ^a p = 0.0001 when compared to the control group for brain cortex CP levels; ^e p = 0.0153 when compared to the control group; ^f p = 0.001, ^g p = 0.027, and ^h p = 0.021 when compared to the AlCl₃ group, for hippocampus CP levels. **(C)** ^a p = 0.0001 when compared to the control group; ^b p = 0.0014, ^c p = 0.0385, and ^d p = 0.0395 when compared to the AlCl₃ group, for brain cortex SOD activity; ^e p = 0.0015 when compared to the control group; ^f p = 0.0084, ^g p = 0.0001, and ^h p = 0.0001 when compared to the AlCl₃ group, for hippocampus SOD activity. **(D)** ^e p = 0.0012 when compared to the control group; ^f p = 0.0064, ^g p = 0.0001, and ^h p = 0.0002 when compared to the AlCl₃ group, for hippocampus CAT activity.

Figure 10. Histological sections of the frontal cerebral cortex (left column) and CA1 region of the hippocampus (right column) **(A)**. Thionine acetate staining method. Arrows indicate degenerating neurons with necrosis appearance. These neurons stain intensely in dark purple and show nuclear degeneration and atrophic cytoplasm. All chrysin treatments promoted a marked reduction in degenerative neurons in both cerebral cortex and hippocampus. Frequency of degenerative neurons in the brain cortex and hippocampus **(B)**. Data are represented as mean \pm SEM. for n = 5 animals per group. Statistical analysis was performed using one-way ANOVA followed by Tukey's test. ^a p = 0.0001 when compared to the control group; ^b p = 0.0001, ^c p = 0.0001, and ^d p = 0.0001 when compared to the AlCl₃ group, for brain cortex necrotic cells frequency. ^e p = 0.0041 when compared to the control group; ^f p = 0.0334, ^g p = 0.0387, and ^h p = 0.0003 when compared to the AlCl₃ group, for hippocampus necrotic cells frequency.

Tables

Tables 1

Primer sequences for quantitative RT-PCR.

Primer	5' to 3' Sequence	
	Forward	Reverse
iNOS	TGAACTACGTCCTGTCCCCT	CTCTTCTCTTGGGTCTCCGC
IL-1 β	TGATGGCTTATTACAGTGGCAATG	GTAGTGGTGGTCGGAGATTCTG
TNF- α	ATCTTCTCGAACCCCGAGTG	GGGTTTGCTACAACATGGGC
B-actin	GCGAGAAGATGACCCAGATC	GGATAGCACAGCCTGGATAG
GAPDH	GGTCGGAGTCAACGGATTTG	GGAAGATGGTGGTGGGATTTC

Table 2

Spontaneous locomotor and exploratory activity in the open field and chimney test of mice

	Open Field (num)	Chimney (s)
	Crossings	Climbing
Control	102.0 \pm 5.30	13.92 \pm 2.08
AlCl ₃	110.8 \pm 11.51	15.70 \pm 3.05
Chrysin 10	109.6 \pm 19.21	16.16 \pm 1.69
Chrysin 30	115.4 \pm 23.35	16.44 \pm 2.08
Chrysin 100	107.8 \pm 12.97	15.14 \pm 2.25

Data are represented as mean \pm SEM for n = 14 -16 animals per group.

Figures

Figure 1

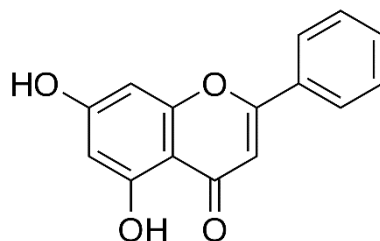


Figure 2

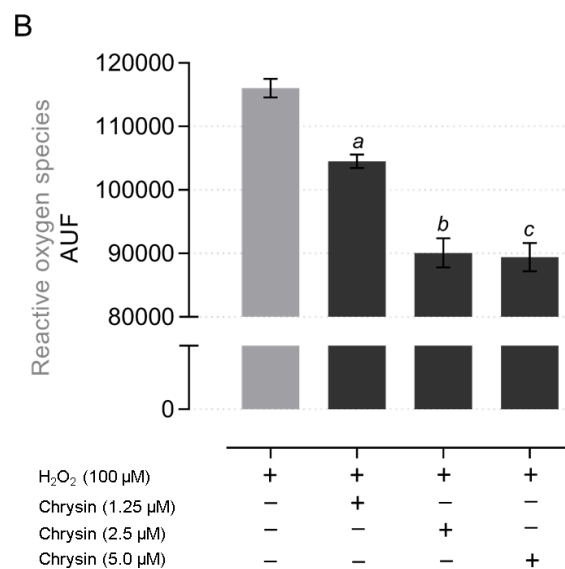
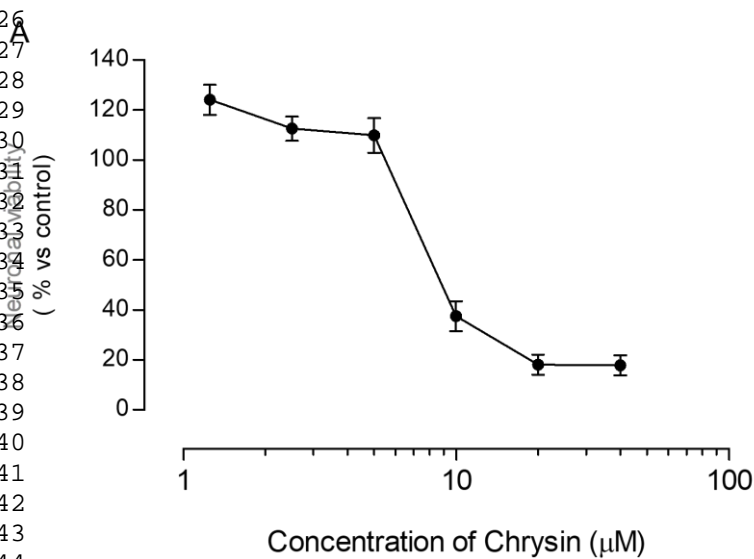
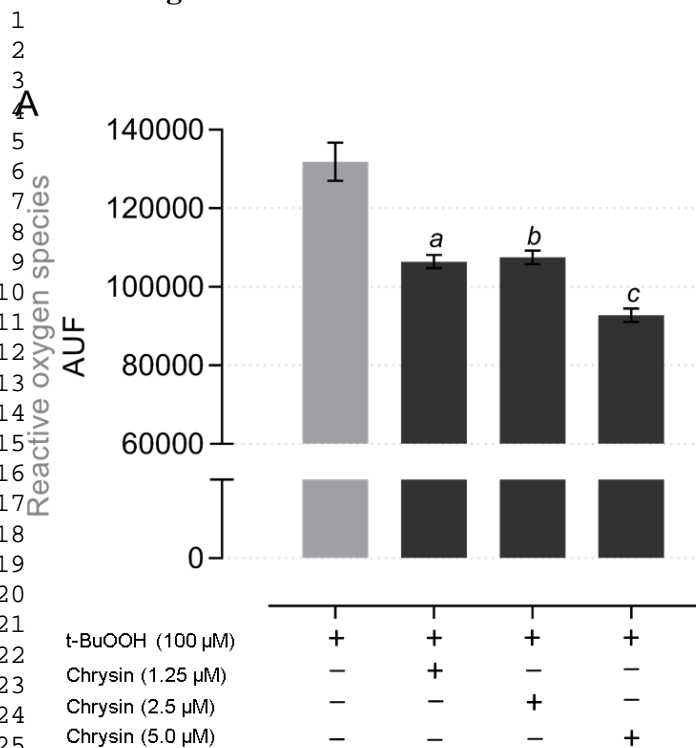


Figure 3

A



B

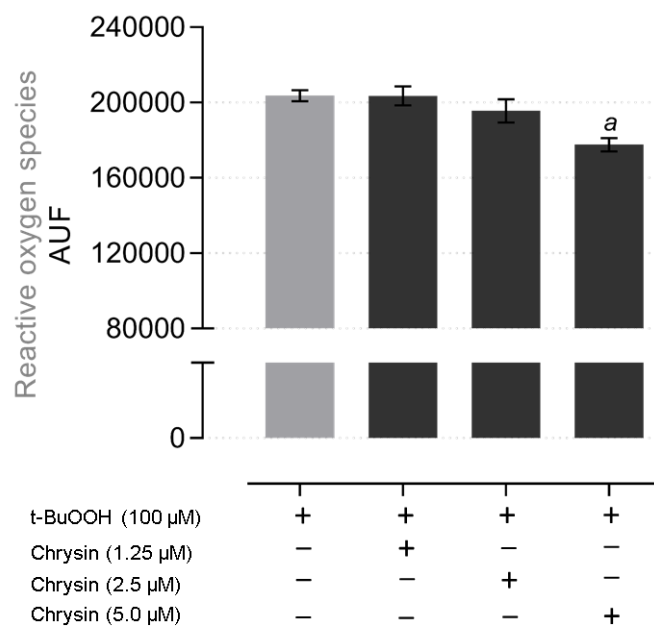
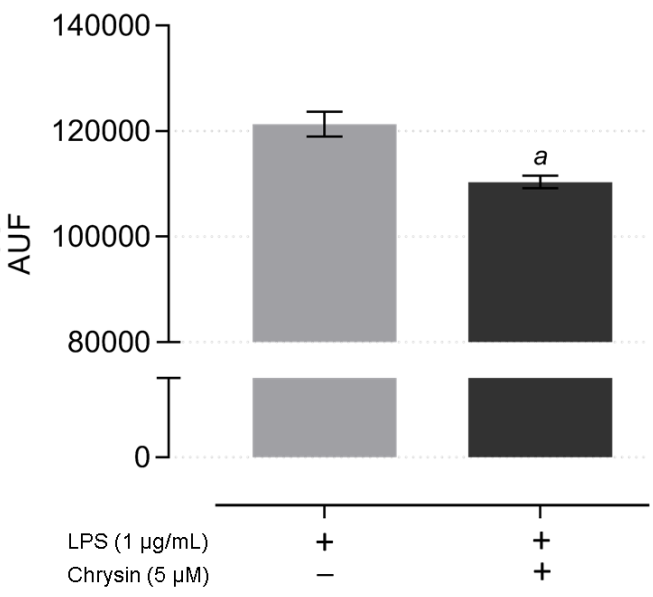


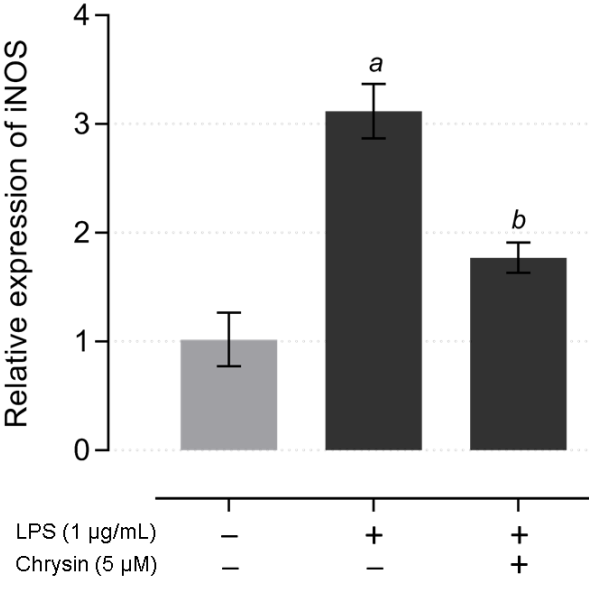
Figure 4

1
2
3
4
5
6
7
8
9
10
11
12
13
14
15
16
17
18
19
20
21
22
23
24
25
26
27
28
29
30
31
32
33
34
35
36
37
38
39
40
41
42
43
44
45
46
47
48
49
50
51
52
53
54
55
56
57
58
59
60
61
62
63
64
65

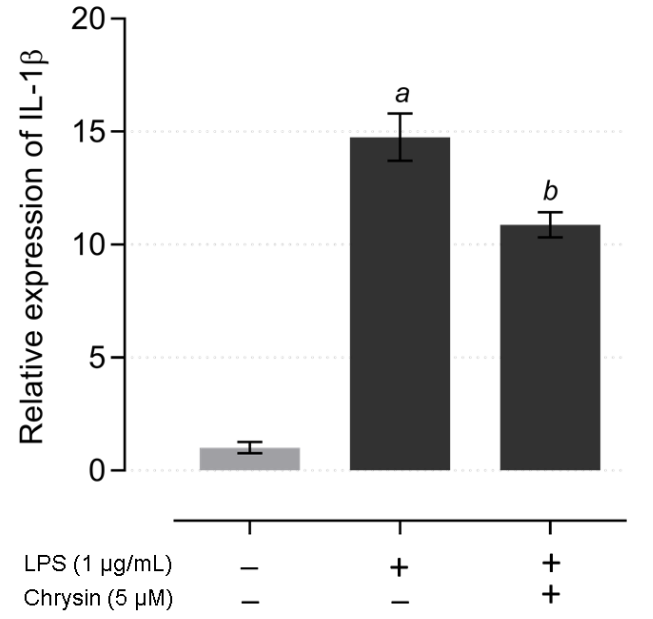
A



B



C



D

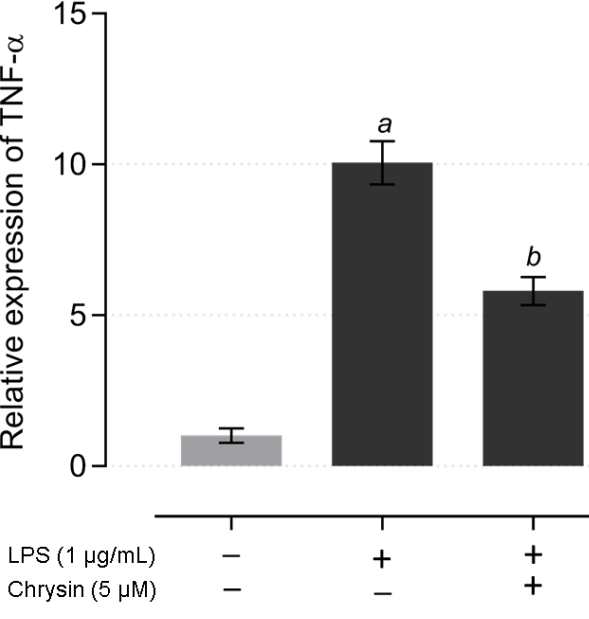


Figure 5

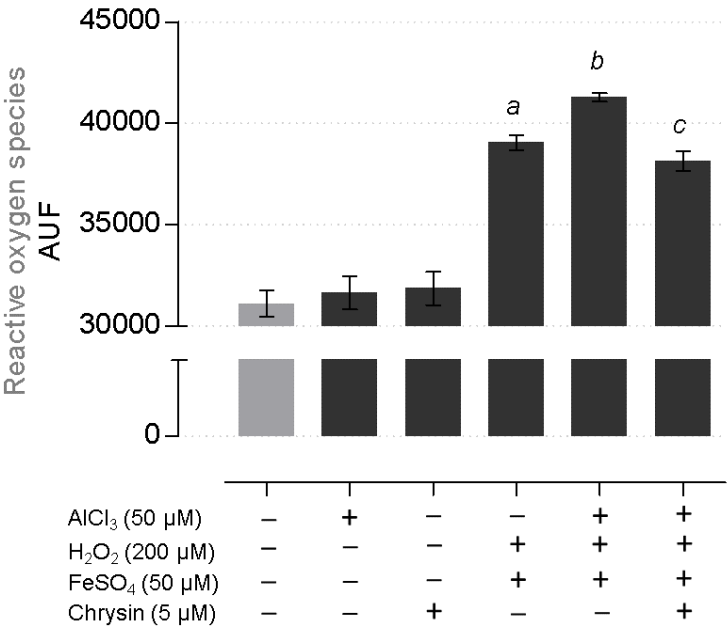


Figure 6

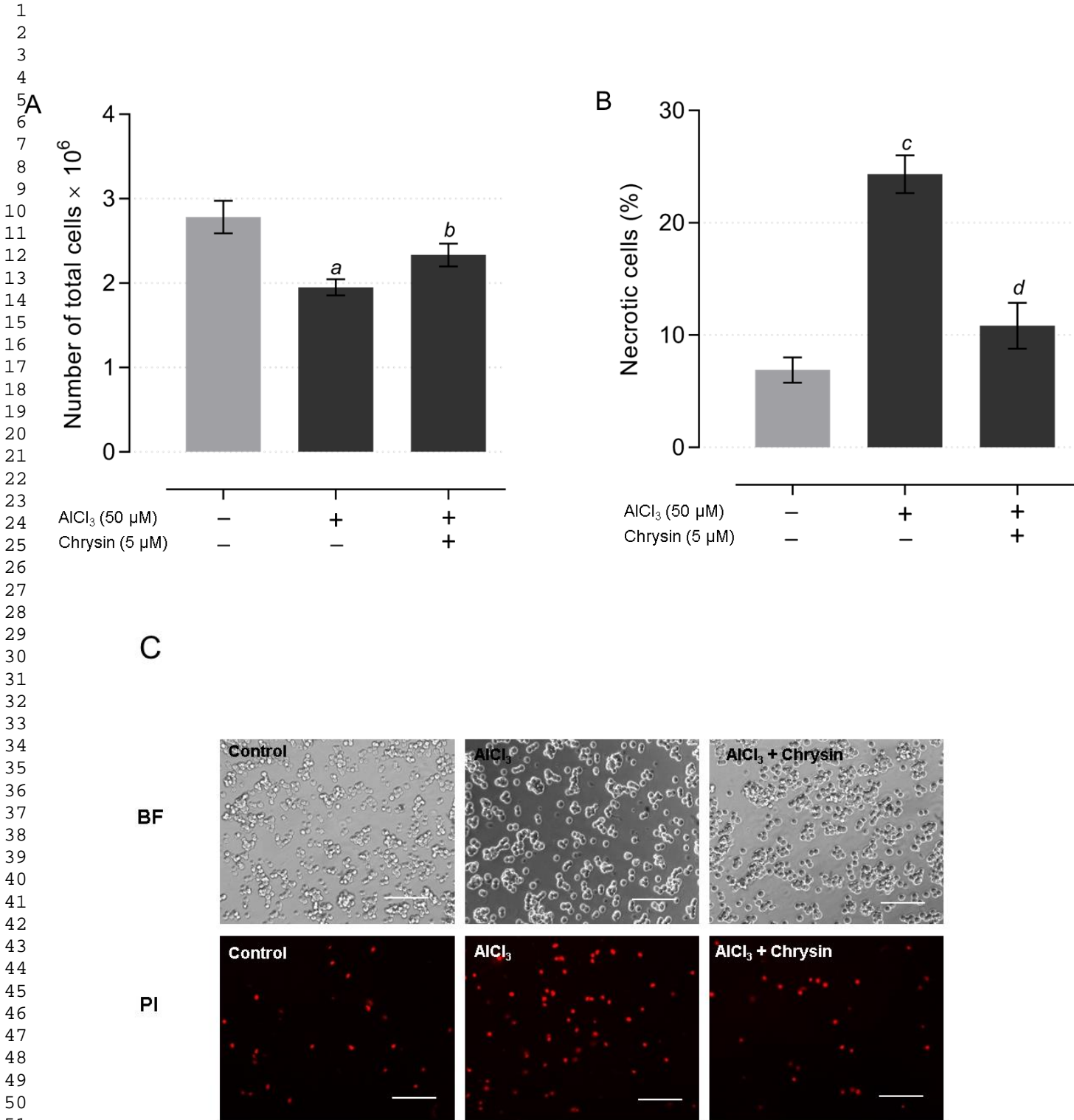


Figure 7

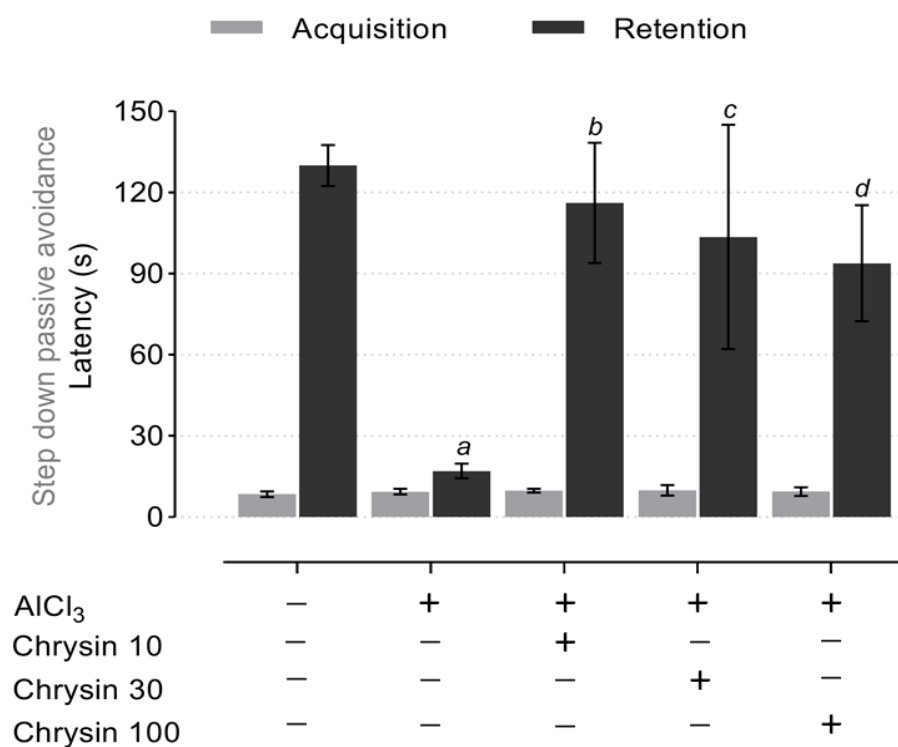


Figure 8

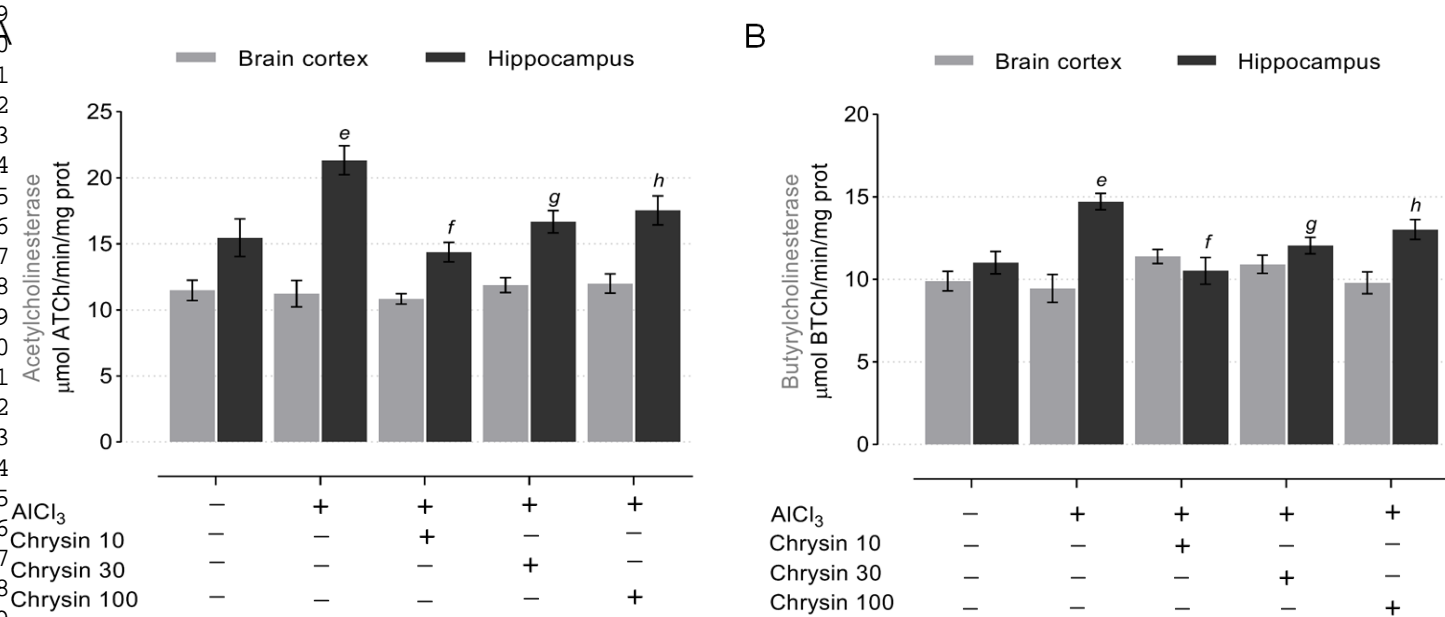


Figure 9

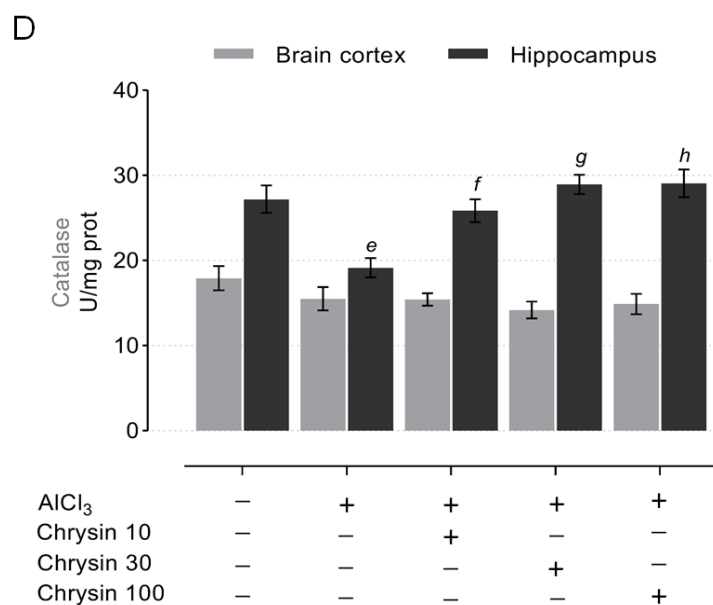
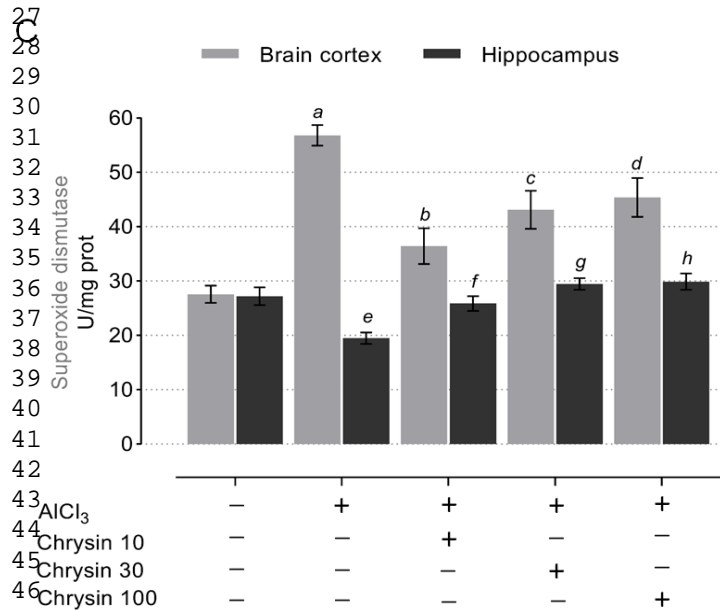
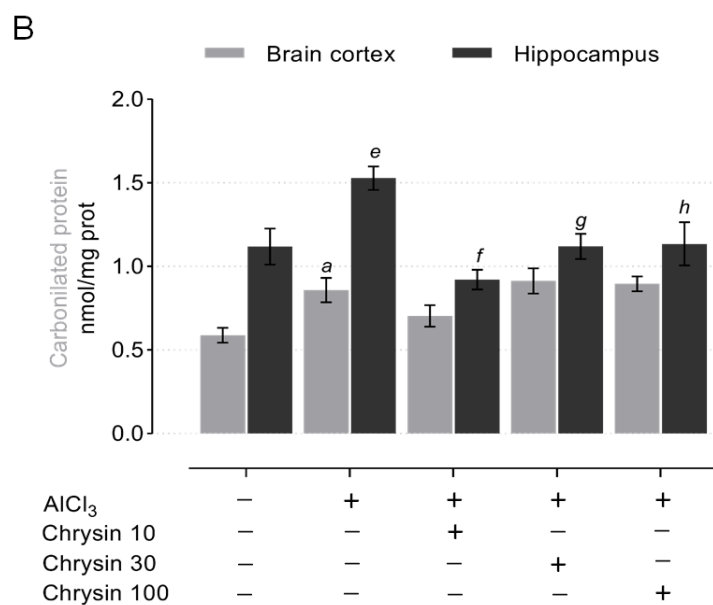
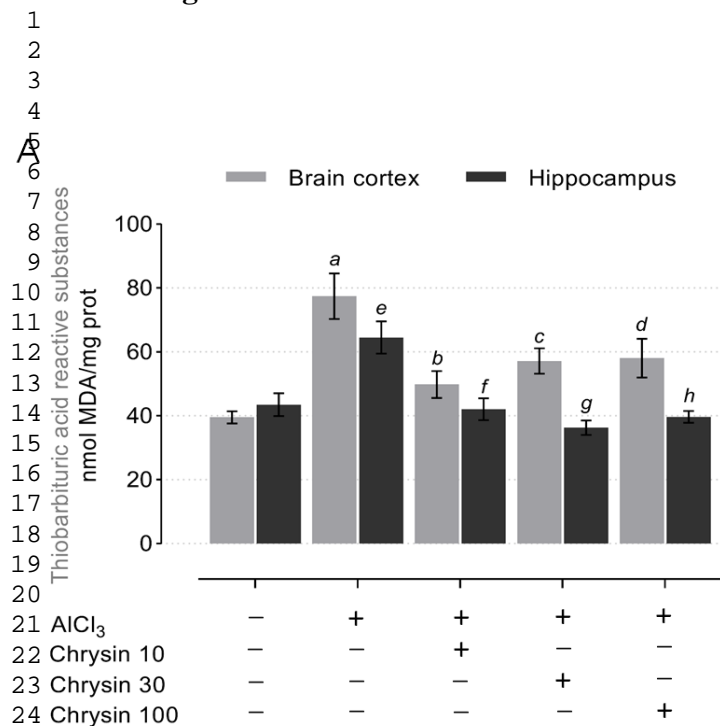
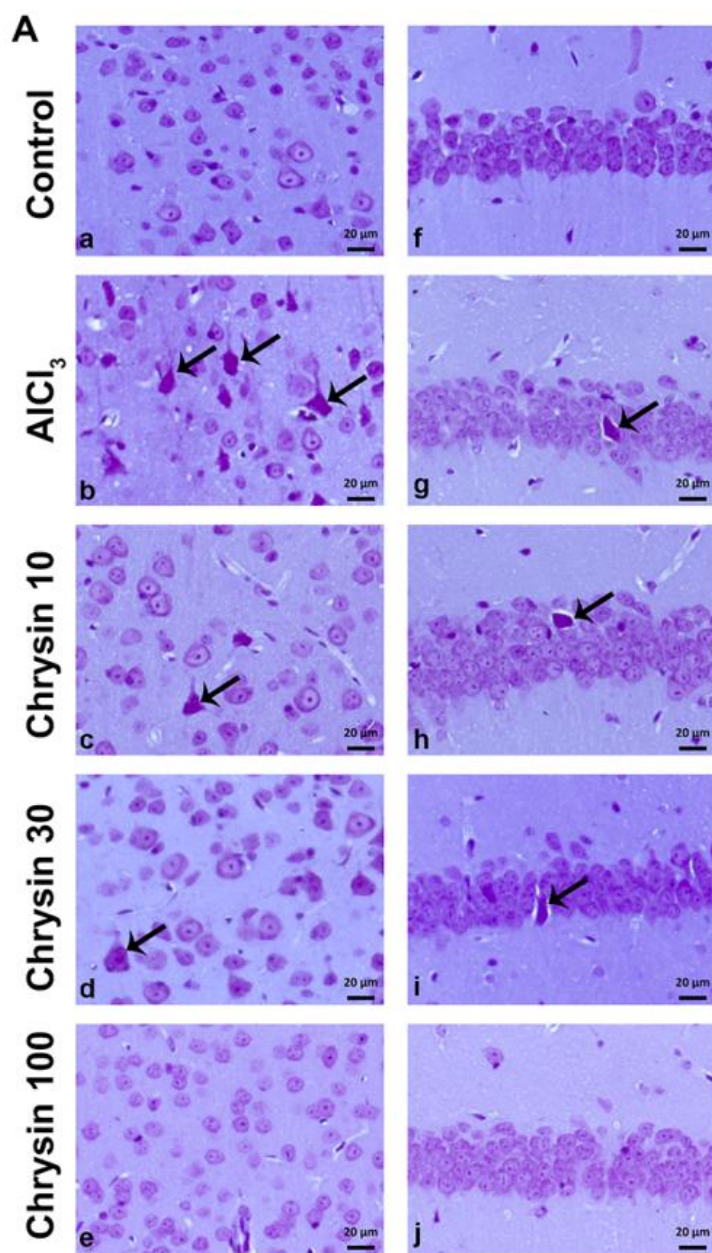


Figure 10



B

